CD4$^+$ T Cells Promote the Transition from Hypertrophy to Heart Failure During Chronic Pressure Overload

Fanny Laroumanie, Victorine Douin-Echinard, Joffrey Pozzo, Olivier Lairez, Claire Vinel, Christine Delage, Denis Calise, Florence Tortosa, Marianne Dutaur, Angelo Parini and Nathalie Pizzinat

The online version of this article, along with updated information and services, is located on the World Wide Web at:

http://circ.ahajournals.org/content/early/2014/03/21/CIRCULATIONAHA.113.007101

Data Supplement (unedited) at:

http://circ.ahajournals.org/content/suppl/2014/03/21/CIRCULATIONAHA.113.007101.DC1.html

CD4^{+} T Cells Promote the Transition from Hypertrophy to Heart Failure During Chronic Pressure Overload

Running title: *Laroumanie et al.; CD4^{+} T cells in chronic heart failure induced by pressure overload*

Fanny Laroumanie, PharmD[1,2]; Victorine Douin-Echinard, PharmD, PhD[1,2]; Joffrey Pozzo, MD[3]; Olivier Lairez, MD, PhD[3]; Claire Vinel, MS[1,2]; Christine Delage, BS[4]; Denis Calise, MS[4]; Florence Tortosa, MS[1,2]; Marianne Dutaur, MS[1,2]; Angelo Parini, MD, PhD[1,2], Nathalie Pizzinat, PhD[1,2]

[1]Institut National de la Santé et de la Recherche Médicale UMR1048 (INSERM), Institute of Cardiovascular and Metabolic Diseases (I2MC), Rangueil, Toulouse; [2]Toulouse III University, Toulouse; [3]Dept of Cardiology, University Hospital of Rangueil, Toulouse; [4]INSERM-UMS 006-Microsurgery Facility, Toulouse, France

Address for Correspondence:

Nathalie Pizzinat, PhD

INSERM UMR-1048

Institut de Médecine Moléculaire de Rangueil, Bât L3

CHU Rangueil

1, Av. J. Poulhès

31403 Toulouse cedex 4, France

Tel: 33 5 31 22 41 20

Fax: 33 5 62 17 25 54

E-mail: nathalie.pizzinat@inserm.fr

1

Abstract

Background—The mechanisms by which the heart adapts to chronic pressure overload, producing a compensated hypertrophy and eventually heart failure (HF) are still not well defined. We aimed to investigate the involvement of T cells in the progression to HF using transverse aortic constriction model (TAC).

Methods and Results—Chronic heart failure was associated with accumulation of T lymphocytes and activated/effector CD4^{+} T cells within cardiac tissue. After TAC, enlarged heart-mediastinal draining lymph nodes showed a high density of both CD4^{+} and CD8^{+} T cell subsets. To investigate the role of T cells in HF, TAC was performed on RAG2KO mice lacking B and T lymphocytes. As compared to WT TAC, RAG2KO mice did not develop cardiac dilation, showed improved contractile function and blunted adverse remodeling. Reconstitution of the T cell compartment into RAG2KO mice prior to TAC enhanced contractile dysfunction, fibrosis, collagen accumulation and cross-linking. To determine the involvement of a specific T cell subset, we performed TAC on mice lacking CD4^{+} (MHCIIKO) and CD8^{+} T cell subsets (CD8KO). In contrast to CD8KO, MHCIIKO did not develop ventricular dilation and dysfunction. MHCIIKO also displayed very low fibrosis, collagen accumulation and cross-linking within cardiac tissue. Interestingly, mice with transgenic CD4^{+} TCR specific for ovalbumin (OT-II) failed to develop HF and adverse remodeling.

Conclusions—These results demonstrate for the first time a crucial role of CD4^{+} T cells and specific antigen recognition in the progression from compensated cardiac hypertrophy to HF.

Key words: heart failure, lymphocytes, remodeling

Introduction

Heart failure (HF) is a complex syndrome that results from acute injury such as myocardial infarction or more long-standing diseases such as pressure and volume overload. In the case of pressure overload conditions, occurring in aortic stenosis or hypertension, cardiac remodeling evolves progressively from an initial compensatory ventricular hypertrophy to decompensated hypertrophy characterized by cardiac dilation and contractile dysfunction. [1] Loss of cardiac function is generally associated to fetal genes reprogramming, aberrant calcium handling, loss of cardiomyocytes and excessive fibrosis. [2][3] To date, the mechanisms responsible for the progression of cardiac remodeling and triggering the transition from cardiac hypertrophy to failure remain unknown.

Many observations provided strong evidence involving inflammation in progression of chronic HF. In particular, high circulating levels of pro-inflammatory mediators (ie: tumor necrosis factor-α and interleukin-6) correlated with deterioration of cardiac function in patients with HF.[4] The importance of these cytokines was further supported by their biological effects on cardiac contractility and remodeling, which may explain several aspects of HF syndrome.[5] Recently, the percentage of circulating $CD4^+$ T cells expressing inflammatory cytokines was positively correlated with the left ventricular dysfunction in patients with HF.[6,7] However, the significance of these observations and the contribution of T cells in cardiovascular remodeling are still poorly understood.

Adaptive cells mediated immunity play an important role in the pathogenesis of inflammatory heart diseases such as myocarditis. In experimental autoimmune myocarditis, T lymphocytes and dendritic cells (DCs) have been demonstrated as obligatory contributors of autoimmune response to tissue damage. [8,9] DCs possess a strong capacity to ingest external

3

antigens and present them through major histocompatibility class II (MHCII) complex to induce CD4^{+} T cell responses.[10] The adoptive transfer of purified T lymphocytes from mice with active myocarditis was sufficient to promote the disease into recipient mice [11,12] underlying the importance of these cells in cardiac dysfunction.

More recently, several lines of evidence have involved T lymphocytes in cardiac remodeling after myocardial infarction. Indeed, reports have shown that modulation of immune cell response by ablation of T cells or DCs altered the initial post infarction healing and remodeling response. By promoting formation of mature collagen matrix and fibrosis, these immune cells may facilitate early wound healing and improved survival post myocardial infarction. [13,14] Although immunity may contribute to different hallmarks of heart failure development, participation of T cells in chronic cardiac remodeling has been poorly addressed in the literature. In the present study, we used complementary mouse models to investigate the role of T lymphocytes in HF progression. Our results showed the key role of CD4^{+} T cells in ventricular remodeling and progression from compensated cardiac hypertrophy to heart failure.

Methods

Detailed methodology is provided in the Data Supplement file.

Animals

Wild type C57BL/6 mice were obtained from Janvier–France. Mice deficient for recombination activating gene 2 expression (RAG2KO) and mice deficient for major histocompatibility complex class II expression (MHCIIKO) due to disruption of the IAβ gene in C57BL/6 were kindly given by Dr van Meerwijk.[15] Mice deficient for CD8α (CD8KO) and OTII mice in which T cells express a TCR specific for OVA in the context of IAβ were from Charles River

4

laboratories. 12-weeks-old male mice were used in all the experiments and were maintained under specific pathogen–free conditions. *In vivo* studies were conducted in mice under European laws on the protection of animals (86/609/EEC). Mouse experiments were approved and performed according to the guidelines of the Ethics and Animal Safety Committee of INSERM Toulouse/ENVT (agreement number : C3155507).

Statistics

All results are presented as mean±SEM. Two group comparisons were analyzed by unpaired 2-tailed *t* test. In the case of nonnormality, the nonparametric test 2-tailed Mann-Whitney U test was used. Multiple group comparisons were performed using the 1-way ANOVA followed by Tukey's post-test. Kruskal and Wallis test followed by Dunn test comparison of pairs was used to analyze data that did not show normal distribution. P values of less than 0.05 were considered significant. All statistical analyses were performed using GraphPad Prism (version 6.01) software.

Results

Chronic Heart Failure is Associated with Cardiac Recruitment of Activated/Effector T cells

In a first set of experiments, we evaluated the expression profile of chemokines implicated in lymphocyte recruitment in cardiac tissue. [16, 17, 18] As shown in **Figure 1-A**, the expression of the chemokines CX3CL1, CXCL16 and CXCL10 was significantly higher in ventricle tissues from TAC induced heart failure than from Sham operated animals. We also observed a strong increase in the expression of CCL17, a chemokine associated with dendritic cells stimulation and involved in attraction of activated T cells. [19] To determine the presence of T cells into cardiac tissue, we performed immunofluorescence analysis. Our results indicated that heart failure is

5

associated with infiltration of T cells into cardiac tissue (**Figure 1-B, 1-C**). To further

characterize T cell subtypes, we performed flow cytometry on the ventricle inflammatory cell

fraction after six weeks of TAC (See gating strategy in **Data Supplement Figure 1**). An

augmentation of ventricular T cells was retrieved after TAC. Indeed, the number of CD4$^+$ and

CD8$^+$ T cells was increased by 3.2-folds and 2.3-folds respectively as compared to Sham mice

(**Figure 1-D**). By immunofluorescence studies, we confirmed the predominance of infiltrated

CD4$^+$ over CD8$^+$ T cells seen in **Figure 1-D** (**Data Supplement Figure 2-A, 2-B**). To further

assess the activation status of these cells, we examined expression level of CD44 to discriminate

activated/effector T cells from their naïve counterpart. Our results showed that the number of

activated/effector CD4$^+$ T cells (CD4$^+$CD44^{hi}) increased in the heart after TAC (**Figure1-E**).

Such rise was not observed for CD8$^+$CD44^{hi} T cells (Data not shown). Among inflammatory

cells, we also observed an accumulation of antigen-presenting cells (identified as CD11c^{hi}

MHCII^{hi} cells, **Data Supplement Figure 3**) within the failing heart.

Chronic Heart Failure is Associated with Increase Cellularity of Mediastinal Draining

Lymph Nodes and Th1 polarization of T cells.

Draining lymph nodes, the epicenter of the immune responses, are dynamic lymphoid structures.

At autopsy, we observed an enlargement of heart-mediastinal draining lymph nodes (MLNs)

associated with a strong increase in total cell number (**Figure 2-A, 2-B**) in mice submitted to

TAC. In addition, cells isolated from MLNs of TAC animals, and stimulated *ex vivo* with anti-

CD3ε anti-CD28 antibodies, secreted higher level of the T cell growth factor IL-2 than cells

isolated from Sham animals (**Figure 2-C**). Moreover analysis by flow cytometry revealed an

increase of CD4$^+$ and CD8$^+$ T cell numbers in MLNs after TAC as compared to Sham animals

(**Figure 2-D**, See gating strategy in **Data Supplement Figure 4**). These results support the

6

enhanced T cell proliferation in lymph nodes after TAC. Differences in lymphocyte subsets after TAC were not observed in spleen (Data not shown).

In order to assess the potential difference in Th1/Th2 polarization, cells isolated from MLNs were stimulated *ex vivo* for 48h by anti-CD3ɛ anti-CD28 antibodies. MLNs cells from TAC group produced more Interferon γ (IFNγ), the Th1 cytokine, after TCR-dependent activation than cells from Sham animals (Sham: 13.05±3.01 vs TAC: 58.95±10.4 ng/ml, *P*<0.01, **Figure 2-E**). In contrast, the level of the Th2 cytokine IL-4 was very low in Sham animals and diminished after TAC (**Figure 2-E**). These results were confirmed by intracellular staining and flow cytometry showing a higher number of IFNγ positive CD4$^+$ and CD8$^+$ T cells after TAC (**Figure 2-F** and **Data Supplement Figure 5**). The percentage of IL-4 positive cells was negligible (below 1%) and unaffected by TAC. Taken together, these results suggest a preferential Th1-type polarization of MLNs T cells.

Absence of B and T Lymphocytes Attenuates the Transition from Hypertrophy to Heart Failure

To determine whether mobilization of lymphocytes in cardiac tissue have an impact on the progression to heart failure, we submitted RAG2KO mice to TAC. RAG2 encodes the Recombination Activation Gene 2 that catalyzes V(D)J recombination, an essential step for the generation of immunoglobulins and T lymphocyte receptors. As a consequence, RAG2KO mice are completely deficient in mature B and T lymphocytes. According to echocardiography parameters (**Table 1**), left ventricular (LV) dimensions and function were similar in wild-type (WT) and RAG2KO mice under unstressed control condition. After 6 weeks of TAC, the absence of lymphocyte prevented cardiac dilation but not ventricular hypertrophy and attenuated cardiac contractile dysfunction induced by pressure overload (**Table 1**).

7

In addition, mRNA expression of the heart failure markers, atrial and brain natriuretic factors (ANF and BNF respectively) was significantly lower in RAG2KO TAC as compared with WT TAC (**Figure 3-A**). Heart failure was also associated with a decrease in SERCA2a expression and a main shift in the myosin heavy chain isoforms, from alpha (MYH6) to beta (MYH7). The decrease in mRNA expression of SERCA2a and MYH6 was attenuated in RAG2KO TAC as compared with WT TAC (**Figure 3-A**). These results indicate that the absence of B and T lymphocytes prevented cardiac dilation and attenuated cardiac dysfunction induced by TAC, suggesting a role of lymphocytes in the transition from hypertrophy to heart failure.

Reconstitution of T Lymphocytes Promotes Pressure Overload induced Heart Failure

To investigate the role of T cells in progression to heart failure, we transferred purified T cells from donor WT mice into RAG2KO mice. After T cell reconstitution, RAG2KO+CD3 and control RAG2KO mice injected with PBS were submitted to TAC. As expected, a strong infiltration of CD3$^+$ T cells detected by immunofluorescence was retrieved in left ventricular tissue of RAG2KO+CD3 after TAC (**Figure 3-B**). T cell reconstitution in RAG2KO mice before surgery produced a significant decrease in cardiac contractility as revealed by reduced fractional shortening (FS) in RAG2KO+CD3 compared with control RAG2KO+PBS mice (FS; RAG2KO+PBS: 24.97±3.4% vs RAG2KO+CD3:16.4±2.0%, *P*<0.05, **Figure 3-C** and **Data Supplement Figure 6**). According to deterioration of contractile function, expression of the heart failure markers ANF and BNF significantly increased in RAG2KO+CD3 compared with RAG2KO+PBS (**Figure 3-D**). Taken together, these results show that T cells contribute to progression of heart failure after TAC.

T Lymphocytes Promote Fibrosis by enhancing collagen accumulation and cross-linking after TAC

Macrophages are known to be involved in inflammatory and fibrotic processes. We observed that TAC induced heart failure was associated with macrophage infiltration (identified as CD68^{+} cells, **Figure 4-A, 4-B**) and excessive perivascular and interstitial fibrosis in cardiac tissue of WT mice (**Figure 4-C, 4-D**). In absence of lymphocytes, both macrophage infiltration (WT TAC: 159±20 vs RAG2KO TAC: 97±12 cells/mm^2, $P<0.05$, **Figure 4-B**) and excessive fibrosis were prevented (WT TAC: 6.5±1.0 vs RAG2KO TAC: 2.2±0.6%, $P<0.01$, **Figure 4-D**).

After T cell replenishment, macrophage density (WT TAC: 159±20; RAG2KO+CD3: 154±13cells/mm^2, **Figure 4-B**) and ventricular fibrosis measured in RAG2KO+CD3 were similar to those found in WT mice (WT TAC: 6.5±1.0; RAG2KO+CD3: 6.43%, **Figure 4-D**). These results support a role of T lymphocytes in deleterious cardiac remodeling seen after six weeks of TAC in WT animals.

In order to gain insight on the mechanisms responsible for the ventricular fibrotic response induced by T cells, we determined the levels of collagen deposition in cardiac tissue by picrosirius red staining. As shown in **Figure 5-A**, RAG2KO mice submitted to TAC presented a significant decrease in collagen content as compared with WT mice. In RAG2KO mice transferred with T lymphocytes, collagen amount was comparable to that observed in WT mice after TAC supporting the involvement of these cells in promoting cardiac collagen accumulation (**Figure 5-B**).

The mRNA expression of the two main procollagens Coll1a1 and Coll3a1 was up regulated after TAC, to a similar extent in both WT and RAG2KO group (**Figure 5-C**). In addition, T cell transfer into RAG2KO mice did not significantly increase the expression of

9

Coll1a1 and Coll3a1 mRNAs (**Figure 5-D**). These results indicate that the profibrotic activity of T lymphocytes involves collagen accumulation by a mechanism independent of procollagen genes expression.

Dysregulation of both collagen deposition and assembling in cross-linked fibers, leading to cardiac fibrosis, is a major determinant of cardiac dysfunction. [20] Recently, Yu et al. [7] suggested that T cells might promote collagen fiber formation by stimulating lysyl oxidase (LOX), an enzyme responsible for collagen cross linking. LOX is produced as an inactive proenzyme (50 kDa) that is cleaved in a shorter active form (32 kDa). In our study, we observed a strong increase in LOX mRNA expression in cardiac tissue of WT mice after TAC (**Figure 6-A**). This phenomenon was associated with an enhanced amount of the pro- and mature forms of LOX, as determined by western blot (**Figure 6-B**). In cardiac tissue of RAG2KO TAC, the increase in LOX mRNA was significantly lower than that observed in WT animals after TAC (**Figure 6-A**). In addition, although the amount of the pro LOX protein was unchanged, the mature LOX was down regulated in RAG2KO after TAC in comparison with Sham (**Figure 6-C**). Reconstitution of T lymphocytes significantly increased LOX mRNA and protein expression in cardiac tissue after TAC mimicking the changes observed in WT mice (**Figure 6-A, 6-D**).

To determine whether LOX modification subsequently affected cross-linked collagen density, we examined collagen fibrils by picrosirius red staining under polarized light.[21] Our results showed the presence of abundant birefringent fibers in WT mice after TAC. Collagen fibers, faintly detectable in RAG2KO mice, were strongly visible in T cell reconstituted mice RAG2KO+CD3 (**Figure 6-E**). Overall, these results indicate that T cells participate in adverse cardiac remodeling after TAC, in part, through the regulation of collagen accumulation and cross linking in heart tissue.

Lack of Functional CD4^{+} but not CD8^{+} T cells Prevented Cardiac Remodeling and Failure in Response to Pressure Overload

In order to define the specific contribution of T cell subsets in pressure overload induced heart failure, we submitted mice lacking functional CD4^{+} T cells (MHCIIKO) and CD8^{+} T cells (CD8KO) to pressure overload. After TAC, MLNs isolated from MHCIIKO mice did not exhibit size increase or higher cellularity in comparison with Sham animals (**Data Supplement Figure 7-A**). In addition, MHCIIKO mice did not develop cardiac dilation after TAC (LVIDd; MHCIIKO Sham: 0.383±0.014 cm vs MHCIIKO TAC: 0.356±0.008 cm, NS, **Table 2**). Although MHCIIKO mice presented myocardial wall thickening after TAC, cardiac contractile function was totally preserved as indicated by unchanged FS compared to Sham (FS; MHCIIKO Sham: 37.61±2.19% vs MHCIIKO TAC: 36.35±2.30%, NS, Table 2). The down regulation of SERCA2a and MYH6 isoform genes, generally observed in heart failure after TAC, was absent in MHCIIKO mice (**Figure 7-A**). In addition, the fact that expression of ANF and BNF was less increased compared to WT TAC further supports the role of CD4^{+} T cells in promoting heart failure (**Figure 7-A**).

The absence of CD4^{+} T cells also prevented adverse remodeling, as seen by largely reduced fibrosis, collagen content and macrophage infiltration after six weeks of TAC (**Figure 7-B, 7-C** and **Data Supplement Figure 8-A**). In addition, the lack of CD4^{+} T cells significantly blunted up-regulation of mRNA and protein expression of LOX and the subsequent collagen fiber formation induced by TAC (**Figure 7-D, 7-E, 7-F**). Taken together, these results highlighted that CD4^{+} T cells are required for the transition from hypertrophy to heart failure.

Next, we performed TAC in CD8KO mice to determine the role of CD8^{+} T cells in progression of heart failure. At autopsy, TAC mice exhibited swollen MLNs with CD4^{+} T cells

11

density very similar to that observed in WT TAC (**Data Supplement Figure 9-A, 9-B**). Echocardiography showed that cardiac function was altered in CD8KO mice after TAC as indicated by a dramatic decrease in the fractional shortening (FS; CD8KO Sham: 37.87±1.53 vs CD8KO TAC: 20.63±2.76, *P*<0.001, **Figure 8-A**) and the development of cardiac dilation (LVIDd; CD8KO Sham: 0.330±0.006 vs CD8KO TAC: 0.388±0.017, *P*<0.05, **Figure 8-A**, **Data Supplement Figure 10**). TAC also modified the mRNA expression of ANF, BNF and SERCA2a in comparison with Sham mice, confirming the severity of cardiac failure (**Data Supplement Figure 11**). Finally, CD8KO mice subjected to TAC presented excessive fibrosis and collagen content as observed in WT mice after TAC (**Figure 8-B**, **Data Supplement Figure 12, 13**). Our results clearly showed that unlike CD4$^+$ T cells, CD8$^+$ T cells are not required for developing chronic heart failure.

To further assess the implication of antigen recognition by the CD4$^+$ T cells, we performed experiments on OT-II mice bearing ovalbumin specific T-cell receptor (TCR). After TAC, these mice did not develop cardiac dilation (LVIDd; OT-II Sham: 0.347±0.013cm vs OT-II TAC: 0.360±0.019cm, NS, **Figure 8-C**, **Data Supplement Figure 14**), showed preserved cardiac function (FS; OT-II Sham: 42.80±3.36% vs OT-II TAC: 35.25±3.77%, NS, **Figure 8-C**, **Data Supplement Figure 14**) and a reduced ventricular fibrosis (OT-II Sham:0.6%±0.6 vs OT-II TAC: 1.8%±0.4, NS, **Figure 8-D**). These findings suggest that deleterious effects of CD4$^+$ T cells depend on antigen recognition.

Discussion

Using combined approaches in different mouse models, we demonstrated here the requirement of CD4$^+$ T cells in the transition from compensated hypertrophy to heart failure.

12

Our results showed that end-stage heart failure (HF) was characterized by an accumulation of both CD4^{+} and CD8^{+} T cells in cardiac ventricles. In agreement with these results, over-expression of chemokines such as CX3CL1, CCL17, CXCL10 and CXCL16 involved in the recruitment and homing of T cells in injured tissues [16,17,22,18] has also been observed during heart failure. The up-regulation of CCL17, mainly expressed by activated DCs in various non lymphoid organs [19] was concomitant with higher cardiac infiltration of DCs in failing heart.

HF was also correlated with robust expansion of heart-mediastinal draining lymph nodes (MLNs), increased number of CD4^{+} and CD8^{+} T cells and elevated secretion of the T cell growth factor IL-2 after *ex vivo* TCR stimulation. These data support T cell proliferation in MLNs during chronic HF. Cytokines production by MLNs T cells assessed after anti-CD3ε /anti-CD28 stimulation, revealed a significant increase in Th1 type cytokine (IFNγ and a decrease in Th2 type cytokine (IL-4) production in mice subjected to TAC. Intracellular staining uncovered the participation of both CD4^{+} and CD8^{+} T cells in IFNγ production. These results are in agreement with observations made in clinical studies describing positive correlation between T cell polarization towards Th1 and the left ventricular dysfunction in patients with HF.[6,23] To date, the relationship between T cell activation and development of chronic HF was poorly defined.

In our current study, we evaluated the participation of T lymphocytes in cardiac remodeling and in transition from hypertrophy to HF by using lymphocyte deficient mice as models. After TAC, heart of RAG2KO mice did not undergo ventricular dilation, exhibited preserved contractile function and showed drastic reduction of fibrosis. Transfer of T lymphocytes, but not B lymphocytes (unpublished data L.F), enhanced contractile dysfunction and promoted adverse ventricular remodeling in RAG2KO following TAC. Although infiltration

13

of both CD4$^+$ and CD8$^+$ T cells was observed in failing heart of WT animals, only CD4$^+$ T cell subset plays a crucial role in cardiac dysfunction. Indeed, MHCIIKO mice lacking mature CD4$^+$ T cells with normal CD8$^+$ T cell compartment [24], were preserved from ventricular dilation and contractile dysfunction and exhibited blunted ventricular fibrosis after TAC. In contrast, CD8KO mice developed cardiac failure and displayed adverse remodeling. Moreover, the fact that higher number of CD8$^+$ T cells was observed within cardiac tissue of MHCIIKO mice after TAC, further argue against a role of this subset in the pathology (**Data Supplement-Figure 7-A, 7-B**). In addition, activated/effector CD4$^+$ T cells infiltration within the failing heart of WT mice emphasized a specific participation of this T cell subset in cardiac dysfunction. As mentioned above, HF was associated with both CD4$^+$ and CD8$^+$ T cells augmentation in MLNs. Interestingly, CD8KO as WT animals had high density of CD4$^+$ T cells in their MLNs while no modification of CD8$^+$ T cell number was retrieved in MHCIIKO mice after TAC (**Data Supplement-Figure 7-A**). This observation suggests that CD4$^+$ T cells may contribute to CD8$^+$ T cell expansion seen in MLNs of WT animals with HF. Taken together, these results show a major role of CD4$^+$ T cell subset in hyperplasia of MLNs associated with HF and in the deterioration of cardiac function during chronic pressure overload.

Our results also showed a striking effect of T cells in fibrotic response induced by pressure overload. Indeed, the significant increase in ventricular fibrosis and collagen deposition observed in WT mice after TAC was not retrieved in RAG2KO mice, lacking T cells. However, T cell transfer induced a similar fibrotic response to that found in WT mice after TAC. This fibrotic process was not affected by the absence of CD8$^+$ T cells but was prevented in mice lacking CD4$^+$ T cell subset. The profibrotic activity of T lymphocytes appeared independent of procollagen gene expression because all groups of mice (WT, RAG2KO, RAG2KO+CD3,

14

CD8KO and MHCIIKO mice) exhibited similarly increase in procollagen I and III mRNA after TAC.

Interestingly, the increase in fibrosis and collagen accumulation was concomitant to enhanced collagen fibers density observed in WT mice after TAC. The assembling into final collagen fibers is a process mediated by LOX enzymes. Moreover, the induction of LOX seems to be a general feature observed in a variety of fibrotic processes in different organs and interestingly has been reported in the fibrotic myocardium of patients with chronic HF.[25,26] In WT mice, LOX expression and ventricular collagen fibers density were increased after TAC whilst these effects were strongly reduced in MHCIIKO and RAG2KO mice. In addition, cardiac contractile dysfunction induced by transfer of T cells into RAG2KO mice was accompanied with up regulation of LOX expression and accumulation of collagen fibers in heart tissue. These results reveal a new contribution of T lymphocytes in fibrosis and collagen accumulation in chronic pressure overload. T cells also participate in cardiac collagen cross-linking, through the induction of LOX expression.

It is noteworthy that, in the case of acute cardiac injury, T lymphocytes seem to have a positive effect by improving wound healing of the myocardium and collagen maturation. [14] These results, along with ours, underline the relevance of T lymphocytes in fibrotic response that could be positive during cardiac repair after acute ischemia and negative during chronic pressure overload. Recently, numerous studies delineated strong implication of IL-17 and IL-1 T cells secreted cytokines in cardiac fibrosis observed in autoimmune heart diseases.[27,28,29] The participation of these cytokines in pressure overload induced HF will deserve further investigations.

The participation of immune system in cardiac remodeling is supported by previous

15

reports describing the beneficial effect of immuno-modulation in hypertensive remodeling. Indeed, sustained Angiotensin II infusion in mice induced hypertrophic cardiac remodeling and increased the number of activated circulating CD4^{+} T subsets. Immunosuppressive treatment of mice by adoptive transfer of regulatory T cells (Tregs) has been shown to attenuate both Angiotensin II induced cardiac fibrosis and hypertrophy. [30] Tregs are a lineage of T cells with anti inflammatory properties and suppressive effects on immune responses. [19] They also strongly reduced ventricular fibrosis with only a small effect on left-ventricular hypertrophy in a mouse model of ventricular pressure overload. [31]

In addition to these previous studies, our results showed that CD4^{+} T cells are required for adverse remodeling and heart failure. The preserved cardiac function of OT-II mice after TAC suggests that the deleterious effect of CD4^{+} T cells is mediated by an inappropriate recognition of antigen. Putative antigens triggering T cell activation have been proposed in cardiac disease. [32] At present, the identity of antigens incriminated in the detrimental effects during pressure overload induced chronic HF remains to be defined.

In conclusion, our results support the concept that T cells, and more specifically CD4^{+} T cell subset, play a crucial role in pressure overload induced cardiac remodeling leading to HF. These cells aggravate tissue remodeling and trigger transition from compensated hypertrophy to HF. Intervention that modulates CD4^{+} T cell activity might represent a novel therapeutic target for the treatment of HF.

Conflict of Interest Disclosures: None.

References:

1. Diwan A, Dorn GW, 2nd. Decompensation of cardiac hypertrophy: cellular mechanisms and novel therapeutic targets. *Physiology (Bethesda).* 2007;22:56-64.

2. Oka T, Komuro I. Molecular mechanisms underlying the transition of cardiac hypertrophy to heart failure. *Circ J.* 2008;72 Suppl A:A13-16.

3. Opie LH, Commerford PJ, Gersh BJ, Pfeffer MA. Controversies in ventricular remodelling. *Lancet.* 2006;367:356-367.

4. Torre-Amione G, Kapadia S, Benedict C, Oral H, Young JB, Mann DL. Proinflammatory cytokine levels in patients with depressed left ventricular ejection fraction: a report from the Studies of Left Ventricular Dysfunction (SOLVD). *J Am Coll Cardiol.* 1996;27:1201-1206.

5. Dahl CP, Husberg C, Gullestad L, Waehre A, Damas JK, Vinge LE, Finsen AV, Ueland T, Florholmen G, Aakhus S, Halvorsen B, Aukrust P, Oie E, Yndestad A, Christensen G. Increased production of CXCL16 in experimental and clinical heart failure: a possible role in extracellular matrix remodeling. *Circ Heart Fail.* 2009;2:624-632.

6. Fukunaga T, Soejima H, Irie A, Sugamura K, Oe Y, Tanaka T, Kojima S, Sakamoto T, Yoshimura M, Nishimura Y, Ogawa H. Expression of interferon-gamma and interleukin-4 production in CD4+ T cells in patients with chronic heart failure. *Heart Vessels.* 2007;22:178-183.

7. Satoh S, Oyama J, Suematsu N, Kadokami T, Shimoyama N, Okutsu M, Inoue T, Sugano M, Makino N. Increased productivity of tumor necrosis factor-alpha in helper T cells in patients with systolic heart failure. *Int J Cardiol.* 2006;111:405-412.

8. Eriksson U, Ricci R, Hunziker L, Kurrer MO, Oudit GY, Watts TH, Sonderegger I, Bachmaier K, Kopf M, Penninger JM. Dendritic cell-induced autoimmune heart failure requires cooperation between adaptive and innate immunity. *Nat Med.* 2003;9:1484-1490.

9. Avlas O, Fallach R, Shainberg A, Porat E, Hochhauser E. Toll-like receptor 4 stimulation initiates an inflammatory response that decreases cardiomyocyte contractility. *Antioxid Redox Signal.* 2011;15:1895-1909.

10. Vyas JM, Van der Veen AG, Ploegh HL. The known unknowns of antigen processing and presentation. *Nat Rev Immunol.* 2008;8:607-618.

11. Smith SC, Allen PM. Myosin-induced acute myocarditis is a T cell-mediated disease. *J Immunol.*1991; 147:2141-2147.

12. Kaya Z, Goser S, Buss SJ, Leuschner F, Ottl R, Li J, Volkers M, Zittrich S, Pfitzer G, Rose NR, Katus HA. Identification of cardiac troponin I sequence motifs leading to heart failure by induction of myocardial inflammation and fibrosis. *Circulation.*2008;118:2063-2072.

13. Anzai A, Anzai T, Nagai S, Maekawa Y, Naito K, Kaneko H, Sugano Y, Takahashi T, Abe H, Mochizuki S, Sano M, Yoshikawa T, Okada Y, Koyasu S, Ogawa S, Fukuda K. Regulatory role of dendritic cells in postinfarction healing and left ventricular remodeling. *Circulation*.2012;125:1234-1245.

14. Hofmann U, Beyersdorf N, Weirather J, Podolskaya A, Bauersachs J, Ertl G, Kerkau T, Frantz S. Activation of CD4+ T lymphocytes improves wound healing and survival after experimental myocardial infarction in mice. *Circulation.* 2012;125:1652-1663.

15. Menager-Marcq I, Pomie C, Romagnoli P, van Meerwijk JP. CD8+CD28- regulatory T lymphocytes prevent experimental inflammatory bowel disease in mice. *Gastroenterology.* 2006;131:1775-1785.

16. Bazan JF, Bacon KB, Hardiman G, Wang W, Soo K, Rossi D, Greaves DR, Zlotnik A, Schall TJ. A new class of membrane-bound chemokine with a CX3C motif. *Nature.*1997;385:640-644.

17. Fife BT, Kennedy KJ, Paniagua MC, Lukacs NW, Kunkel SL, Luster AD, Karpus WJ. CXCL10 (IFN-gamma-inducible protein-10) control of encephalitogenic CD4+ T cell accumulation in the central nervous system during experimental autoimmune encephalomyelitis. *J Immunol.* 2001;166:7617-7624.

18. Jansson AM, Aukrust P, Ueland T, Smith C, Omland T, Hartford M, Caidahl K. Soluble CXCL16 predicts long-term mortality in acute coronary syndromes. *Circulation.* 2009;119:3181-3188.

19. Alferink J, Lieberam I, Reindl W, Behrens A, Weiss S, Huser N, Gerauer K, Ross R, Reske-Kunz AB, Ahmad-Nejad P, Wagner H, Forster I. Compartmentalized production of CCL17 in vivo: strong inducibility in peripheral dendritic cells contrasts selective absence from the spleen. *J Exp Med.* 2003;197:585-599.

20. Goldsmith EC, Bradshaw AD, Spinale FG. Cellular mechanisms of tissue fibrosis. 2. Contributory pathways leading to myocardial fibrosis: moving beyond collagen expression. *Am J Physiol Cell Physiol.* 2013;304:C393-402.

21. Bradshaw AD, Baicu CF, Rentz TJ, Van Laer AO, Boggs J, Lacy JM, Zile MR. Pressure overload-induced alterations in fibrillar collagen content and myocardial diastolic function: role

of secreted protein acidic and rich in cysteine (SPARC) in post-synthetic procollagen processing. *Circulation.* 2009;119:269-280.

22. Heiseke AF, Faul AC, Lehr HA, Forster I, Schmid RM, Krug AB, Reindl W. CCL17 promotes intestinal inflammation in mice and counteracts regulatory T cell-mediated protection from colitis. *Gastroenterology.* 2012;142:335-345.

23. Yndestad A, Holm AM, Muller F, Simonsen S, Froland SS, Gullestad L, Aukrust P. Enhanced expression of inflammatory cytokines and activation markers in T-cells from patients with chronic heart failure. *Cardiovasc Res.* 2003;60:141-146.

24. Madsen L, Labrecque N, Engberg J, Dierich A, Svejgaard A, Benoist C, Mathis D, Fugger L. Mice lacking all conventional MHC class II genes. *Proc Natl Acad Sci U S A.* 1999;96:10338-10343.

25. Maki JM. Lysyl oxidases in mammalian development and certain pathological conditions. *Histol Histopathol.* 2009;24:651-660.

26. Gonzalez A, Ravassa S, Beaumont J, Lopez B, Diez J. New targets to treat the structural remodeling of the myocardium. *J Am Coll Cardiol.* 2011;58:1833-1843.

27. Blyszczuk P, Kania G, Dieterle T, Marty RR, Valaperti A, Berthonneche C, Pedrazzini T, Berger CT, Dirnhofer S, Matter CM, Penninger JM, Luscher TF, Eriksson U. Myeloid differentiation factor-88/interleukin-1 signaling controls cardiac fibrosis and heart failure progression in inflammatory dilated cardiomyopathy. *Circ Res.* 2009;105:912-920.

28. Baldeviano GC, Barin JG, Talor MV, Srinivasan S, Bedja D, Zheng D, Gabrielson K, Iwakura Y, Rose NR, Cihakova D. Interleukin-17A is dispensable for myocarditis but essential for the progression to dilated cardiomyopathy. *Circ Res.* 2010;106:1646-1655.

29. Saxena A, Chen W, Su Y, Rai V, Uche OU, Li N, Frangogiannis NG. IL-1 induces proinflammatory leukocyte infiltration and regulates fibroblast phenotype in the infarcted myocardium. *J Immunol.* 2013;191:4838-4848.

30. Kvakan H, Kleinewietfeld M, Qadri F, Park JK, Fischer R, Schwarz I, Rahn HP, Plehm R, Wellner M, Elitok S, Gratze P, Dechend R, Luft FC, Muller DN. Regulatory T cells ameliorate angiotensin II-induced cardiac damage. *Circulation.* 2009;119:2904-2912.

31. Kanellakis P, Dinh TN, Agrotis A, Bobik A. CD4(+)CD25(+)Foxp3(+) regulatory T cells suppress cardiac fibrosis in the hypertensive heart. *J Hypertens.* 2011;29:1820-1828.

32. Wehlou C, Delanghe JR. Detection of antibodies in cardiac autoimmunity. *Clin Chim Acta.* 2009;408:114-122.

Table 1. Absence of lymphocytes in RAG2KO mice prevents cardiac dilation and attenuated cardiac dysfunction induced by 6 weeks of TAC. Echocardiographic parameters of WT and RAG2KO mice after TAC.

	WT	WT		RAG2KO	RAG2KO	
	Sham n=10	**TAC** n=20	***P***	**Sham** n=10	**TAC** n=17	***P***
IVSd (cm)	0.083±0.008	0.109±0.003	***	**0.086±0.002**	**0.107±0.004**	****, NS**
LVPWd (cm)	**0.080±0.008**	**0.106±0.006**	*	**0.087±0.002**	**0.103±0.006**	***, NS**
LVIDd (cm)	0.383±0.012	0.460±0.014	***	0.362±0.012	0.395±0.009	**NS, †††**
LVIDs (cm)	**0.260±0.029**	**0.382±0.018**	***	**0.247±0.003**	**0.298±0.012**	**NS, †††**
EDV (ml)	0.148±0.019	0.248±0.020	***	0.121±0.012	0.160±0.010	**NS, †††**
ESV (ml)	**0.052±0.008**	**0.155±0.019**	***	**0.050±0.002**	**0.073±0.008**	**NS, †††**
FS (%)	32.17±3.40	17.70±1.67	**	31.71±2.74	24.82±1.85	***, †**
HR (BMP)	532±18	581±29	NS	536±14	543±17	**NS, NS**

IVSd indicates diastolic interventricular septal wall thickness; LVPWd, diastolic left posterior wall thickness; LVIDd, diastolic left ventricular dimension; LVIDs, systolic left ventricular dimension; EDV, end diastolic volume; ESV, end systolic volume; FS, fractional shortening and HR, heart rate. Values shown are mean±SEM. Significance vs corresponding Sham group: *P<0.05, **P<0.01, ***P<0.001. Significance vs WT TAC: †P<0.05, †††P<0.001 by ANOVA.

Table 2. Absence of CD4^{+} T cells in MHCIIKO mice prevents cardiac dilation and dysfunction induced by 6 weeks of TAC. Echocardiographic parameters of WT and MHCIIKO mice after TAC.

	WT	WT		MHCII-KO	MHCII-KO	
	Sham n=9	**TAC** n=18	***P***	**Sham** n=10	**TAC** n=21	***P***
IVSd (cm)	0.082±0.01	0.110±0.004	**	0.085±0.003	0.107±0.004	****, NS**
LVPWd (cm)	**0.080±0.004**	**0.109±0.006**	*	**0.086±0.005**	**0.102±0.005**	***, NS**
LVIDd (cm)	0.380±0.046	0.452±0.013	***	0.383±0.014	0.356±0.008	**NS, †††**
LVIDs (cm)	**0.247±0.031**	**0.377±0.018**	***	**0.241±0.016**	**0.228±0.011**	**NS, †††**
EDV (ml)	0.140±0.019	0.241±0.02	***	0.150±0.017	0.117±0.008	**NS, †††**
ESV (ml)	**0.044±0.006**	**0.155±0.021**	***	**0.042±0.01**	**0.036±0.005**	**NS, †††**
FS (%)	35.13±4.56	17.47±2.0	***	37.61±2.19	36.35±2.30	**NS, †††**
HR (BMP)	**526±20**	**558±23**	**NS**	**560±10**	**579±7**	**NS, NS**

Values shown are mean±SEM. Significance vs corresponding Sham group: *P<0.05, **P<0.01, ***P<0.001. Significance vs WT TAC: †††P<0.001 by ANOVA.

Figure Legends:

Figure 1. Chronic heart failure induced by transverse aortic constriction (TAC) is associated with cardiac T lymphocyte infiltration. (A) Cardiac mRNA expression of chemokines implicated in lymphocyte recruitment: CX3CL1, CXCL16, CXCL10 and CCL17 in Sham and TAC operated mice (n=6-12 per group). mRNA expression was normalized to GAPDH and represented as fold change to Sham. (B) Co-staining by immunofluorescence of $CD3^+$ (T cell marker in red) and $CD45^+$ cells (pan leukocyte marker in green) in cardiac tissue after TAC. Merged image illustrates co-expression and nuclei were stained by DAPI (blue color). Bar corresponds to 10µm. (C) Quantification of immunohistochemical CD3 positive cells in cardiac tissue of Sham and mice submitted to TAC (n=5). (D) Representative flow cytometry dot plots and quantification of T cells ($CD3^+ TCR_\beta^+$) and $CD4^+$ ($CD3^+ TCR_\beta^+ CD4^+$) and $CD8^+$ ($CD3^+ TCR_\beta^+ CD8^+$) T cell subsets isolated from cardiac tissue of Sham and TAC operated mice (n=5-9). (E) Flow cytometry dot plots represented $CD44^+$ and TCR_β^+ expression in $CD4^+$T cells previously gated on $CD45^+/TCR_\beta^+/CD3^+/CD4^+$. Quantification of $CD4^+CD44^{hi}$ cells was expressed as number of cell per heart. Values shown are mean±SEM. Significance vs Sham: *$P<0.05$, **$P<0.01$, ***$P<0.001$ by *t* test (Figure 1A, C, E) or *U* test (D).

Figure 2. Mediastinal heart draining lymph nodes (MLNs) from mice submitted to TAC exhibit activation and modification of T lymphocyte subsets. (A) Gross photograph of MLNs freshly isolated from Sham and mice submitted to TAC. Bar corresponds to 2mm. (B) Quantification of cellular density of MLNs expressed as cell number per MLNs isolated from Sham and TAC operated mice (n=8). (C) Level of Interleukin-2 (IL-2) in culture supernatant of MLNs cells after

21

ex vivo restimulation (n=6). (D) Quantification by flow cytometry of T cells (CD3$^+$TCR$_\beta^+$), CD4$^+$ and CD8$^+$ T cells. Results were expressed in number of cells per MLNs. (E) Levels of Interferon γ (IFNγ) and Interleukin 4 (IL-4) in culture supernatant of MLNs cells after *ex vivo* restimulation (n=6). (F) Quantification by flow cytometry of IFNγ positive CD4$^+$ and CD8$^+$ T cells in MLNs isolated from Sham and TAC operated animals after *ex vivo* stimulation. Values shown are mean±SEM. Significance vs Sham: *P<0.05, **P<0.01 by *U* test.

Figure 3. Deleterious effect of T lymphocyte reconstitution on cardiac function during TAC. (A) Cardiac mRNA expression of atrial and brain natriuretic peptides (ANF, BNF), α and β myosin heavy chains (MYH6, MYH7) and the sarco(endo) plasmic reticulum Ca^{2+}ATPase (SERCA2a) of WT and RAG2KO mice (n=10). mRNA expression was normalized to GAPDH and represented as fold change to WT Sham. (B) Immunofluorescence of the T cell marker CD3 (red) and the pan leukocyte marker CD45 (green) in cardiac tissue of RAG2KO mice reconstituted with CD3 (RAG2KO+CD3) after TAC. Merged image illustrate co-expression and nuclei were stained by DAPI (blue color). (C) Fractional shortening (FS) of RAG2KO mice reconstituted with T lymphocytes (RAG2KO+CD3, n=6) and control (RAG2KO+PBS, n=7) after 6 weeks of TAC. (D) Cardiac mRNA expression of the atrial and brain natriuretic peptides (ANF, BNF) after 6 weeks of TAC (n=6-7). Expression was normalized to RAG2KO+PBS. Values shown are mean±SEM. Significance vs Sham: *P<0.05, **P<0.01, ***P<0.001. Significance vs WT TAC: $^\dagger P$<0.05, $^{\dagger\dagger}P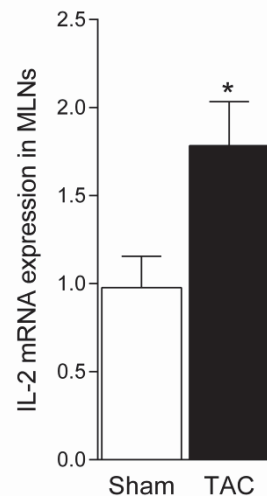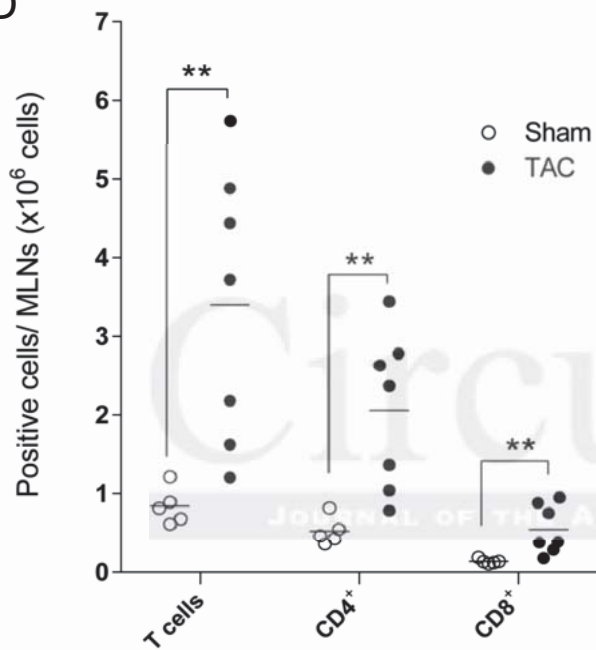$<0.01, $^{\dagger\dagger\dagger}P$<0.001 by ANOVA (Figure 3A). Significance vs RAG2KO+PBS: $^*P$<0.05 by *U* test (C) or *t* test (D).

Figure 4. T lymphocytes play major role in macrophage infiltration and excessive fibrosis after

22

TAC. (A) Representative staining of macrophages with anti-CD68 antibody (arrows) in cardiac tissue of WT, RAG2KO, RAG2KO+PBS and RAG2KO+CD3 mice after TAC. (B) Quantification of CD68 positive cells per mm^2 in WT (n=10), RAG2KO (n=10), RAG2KO+PBS (n=7) and RAG2KO+CD3 (n=6). (C) Representative transverse sections of whole mouse heart subjected to TAC for 6 weeks and stained with Masson's trichrome. Bottom images show enlarged portion of heart section. Scale bar corresponds to 1mm. (D) Quantification of fibrosis in slides as (C) (n=10 for WT and RAG2KO, n=7 for RAG2KO+PBS and n=6 RAG2KO+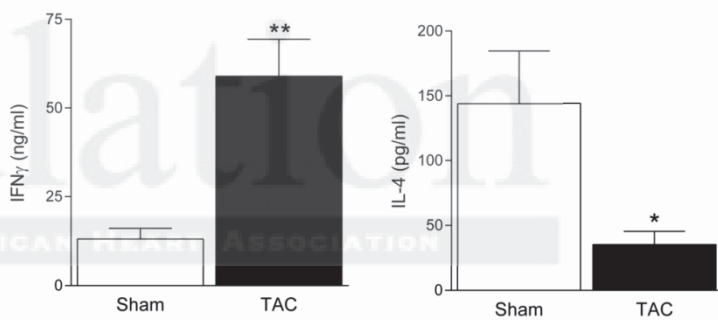CD3). Values shown are mean±SEM. Significance vs WT Sham: ***P<0.001. Significance vs WT TAC: †P<0.01, ††P<0.01. Significance vs RAGKO+PBS: #P<0.05, ANOVA.

Figure 5. T lymphocytes increase collagen content but do not modify pro-collagens expression after TAC. Collagen deposition in cardiac tissue of WT, RAG2KO (A), RAG2KO+PBS and RAG2KO+CD3 mice, (B) submitted to TAC based on picrosirius red staining viewed under white light. Quantification of total collagen deposition in cardiac tissue of WT and RAG2KO and of RAG2KO+PBS and RAG2KO+CD3 mice. (C) Cardiac mRNA expression of type I and III procollagens (Coll1a1 and Coll3a1) in WT and RAG2KO mice (n=10) and (D) in RAG2KO+PBS (n=7) and RAG2KO+CD3 (n=6). Data were normalized to GAPDH and calibrated to the average of WT Sham (B) or RAG2KO+PBS (C). Values shown are mean±SEM. Significance vs Sham or WT TAC: *P<0.05, **P<0.01. Significance vs RAG2KO+PBS: ##P<0.01 by t test (Figure 5A, B, D) or ANOVA (C).

Figure 6. T lymphocytes enhance up-regulation of collagen cross linking enzyme lysyl oxidase (LOX) induced by TAC. (A) Cardiac mRNA expression of LOX in WT and RAG2KO (n=10)

23

and in RAG2KO+PBS (n=7) and RAG2KO+CD3 (n=6) mice after TAC Data were normalized to GAPDH and calibrated to the average of WT Sham. (B) Representative immunoblots and quantitative analysis of pro-LOX protein (50 kDa) and mature LOX protein (32 kDa) expression in WT, (C) RAG2KO and (D) RAG2KO+CD3 (n=4 per group). Results were normalized to GAPDH and expressed as fold over corresponding controls. (E) Collagen fibers observed after picrosirius red–staining under polarized light in cardiac tissue of WT, RAG2KO+PBS and RAG2KO+CD3 mice after TAC (x200). Values shown are mean±SEM. Significance vs Sham: *P<0.05, **P<0.01, ***P<0.001. Significance vs WT TAC: [†]P<0.05. Significance vs RAGKO+PBS: [#]P<0.05 by ANOVA (Figure 6A) or U test (B, D) or t test (C).

Figure 7. Absence of CD4^{+} T cell (MHCIIKO mice) prevents fetal genes activation and adverse cardiac remodeling induced by TAC. (A) Cardiac mRNA expression of ANF, BNF as well as MYH6, MYH7 and SERCA2a in WT and MHCIIKO mice (Sham, n=6; TAC, n=13). (B) Quantification of fibrotic areas after Masson's trichrome staining in cardiac tissue of WT and MHCIIKO mice after TAC (n=8). (C) Quantification of total collagen deposition in cardiac tissue of WT and MHCIIKO mice submitted to TAC based on picrosirius red staining viewed under white light (n=8). (D) Cardiac mRNA expression of LOX (n=6-13). Data were normalized to GAPDH and calibrated to the average of WT Sham. (E) Representative immunoblot for LOX in cardiac tissue of MHCIIKO mice and quantitative analysis of pro-LOX protein (50 kDa) and mature LOX protein (32 kDa) expression (n=4 per group). Results were expressed as fold over corresponding Sham. (F) Picrosirius red–stained sections (observed in C) viewed under polarized light in cardiac tissue of WT and MHCIIKO mice after TAC (x200). Values shown are mean±SEM. Significance vs Sham: *P<0.05, **P<0.01, ***P<0.001. Significance vs WT TAC: [†]P<0.05, [††]P<0.01, [†††]P<0.001 by ANOVA (Figure 7A, B, D) or U test (C, E).

24

25

Figure 8. Contrary to CD8KO mice, T-cell receptor transgenic OTII mice were prevented from chronic heart failure. (A) Diastolic left ventricular dimension (LVIDd) and fractional shortening (FS) were evaluated in WT (n=7-13) and CD8KO (n=5-8) after 6 weeks of TAC. (B) Quantification of fibrotic areas after Masson's trichrome staining in cardiac tissue of WT and CD8KO mice after TAC (n=4-8). (C) LVIDd and FS were evaluated in WT (n=8-9) and OTII mice (n=4-8) after TAC. (D) Quantification of fibrotic areas in cardiac tissue of WT and OTII mice after TAC. Values shown are mean±SEM. Significance vs Sham: *P<0.05, **P<0.01, ***P<0.001; significance vs WT TAC: ††P<0.01: †††P<0.001 by ANOVA.

Figure 1

Figure 2

A

Figure 3

B

C

D

Figure 4

Figure 5

Figure 6

A

B

C

D

E

Figure 7

Figure 8
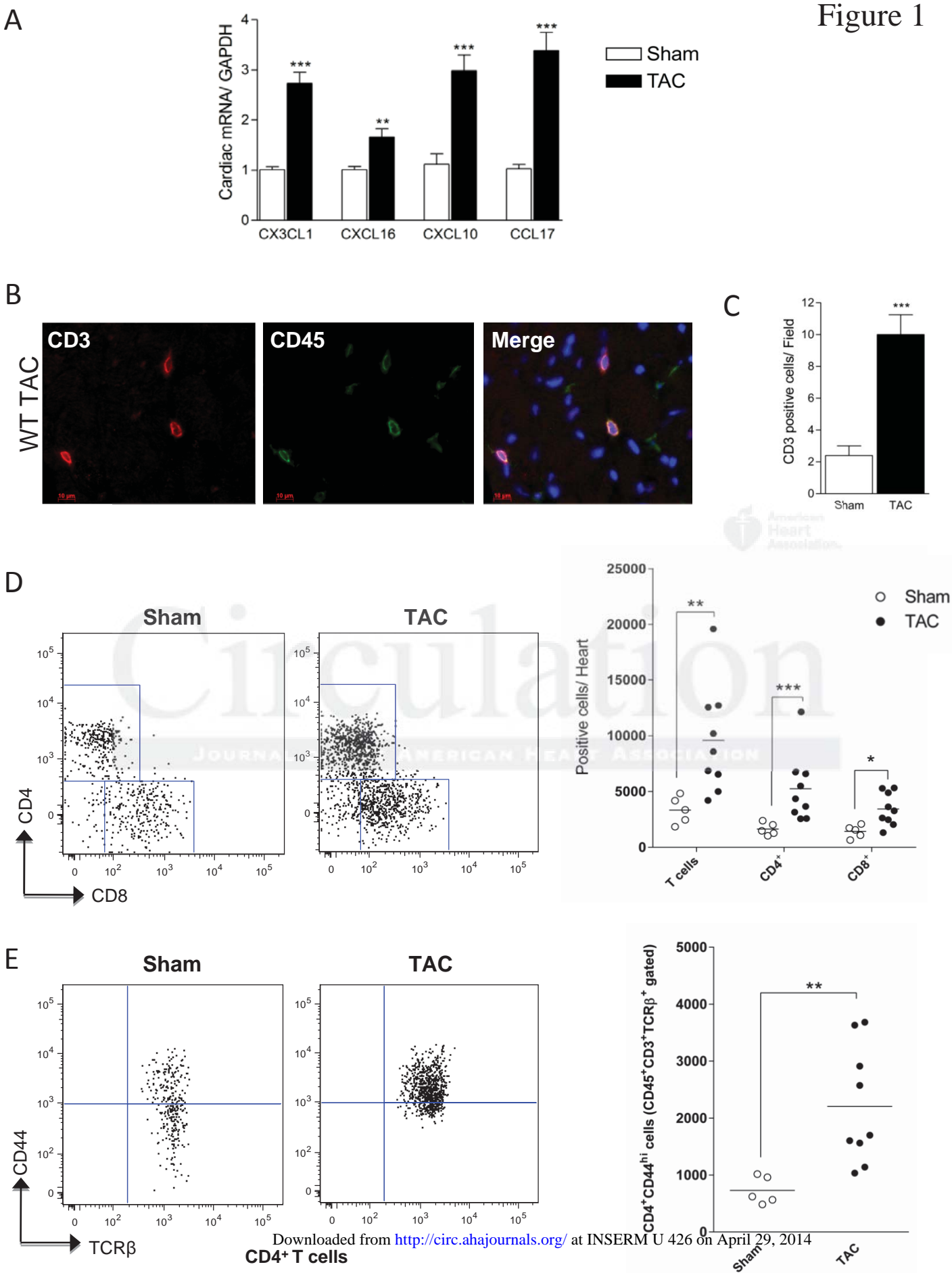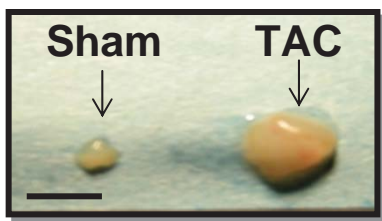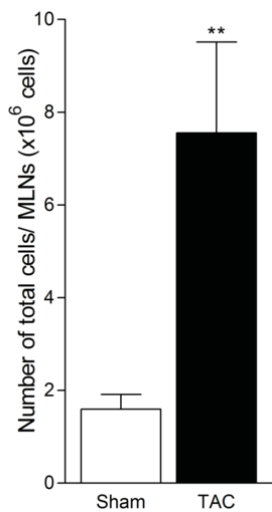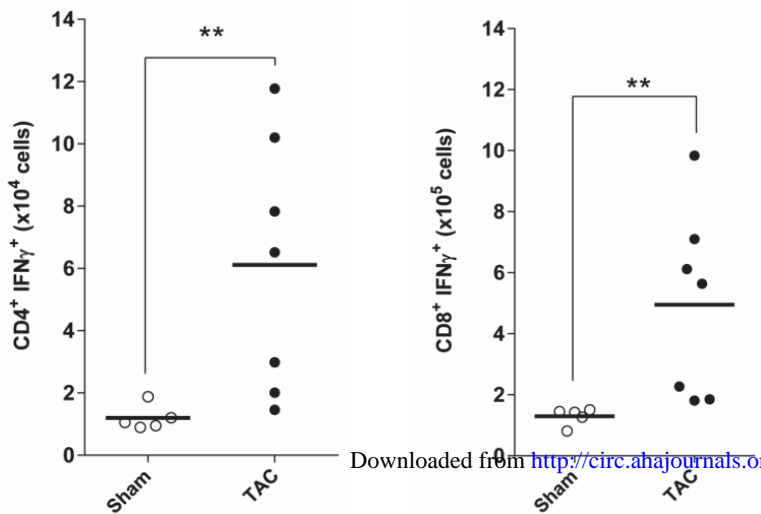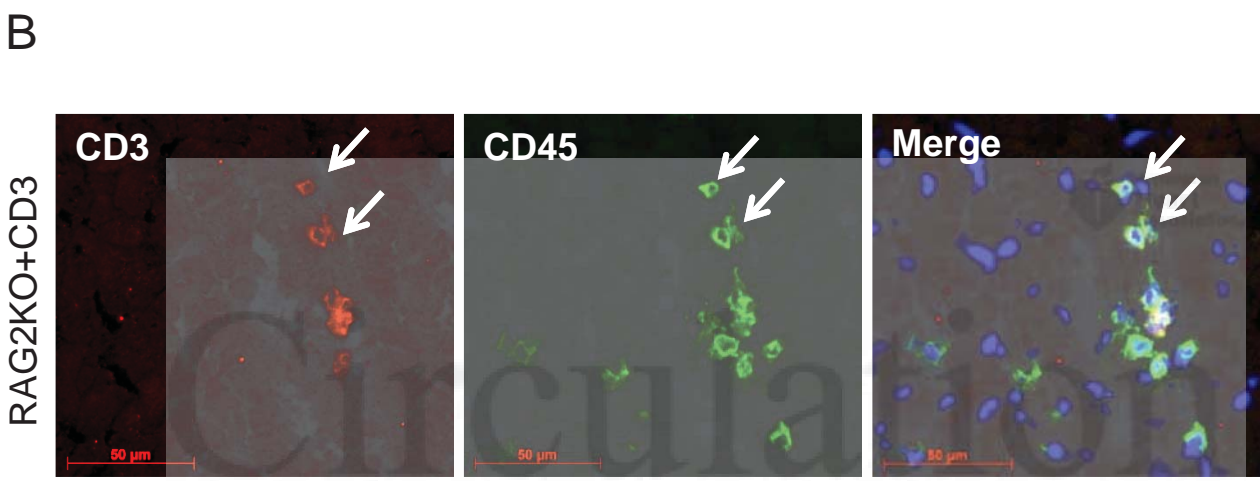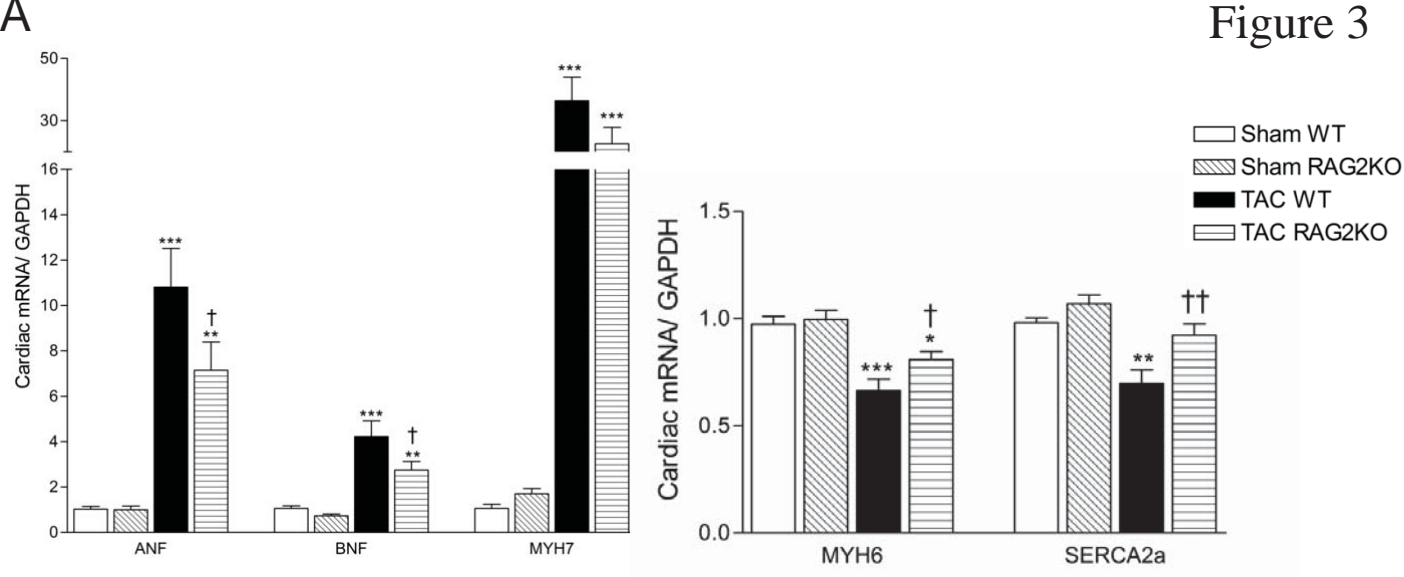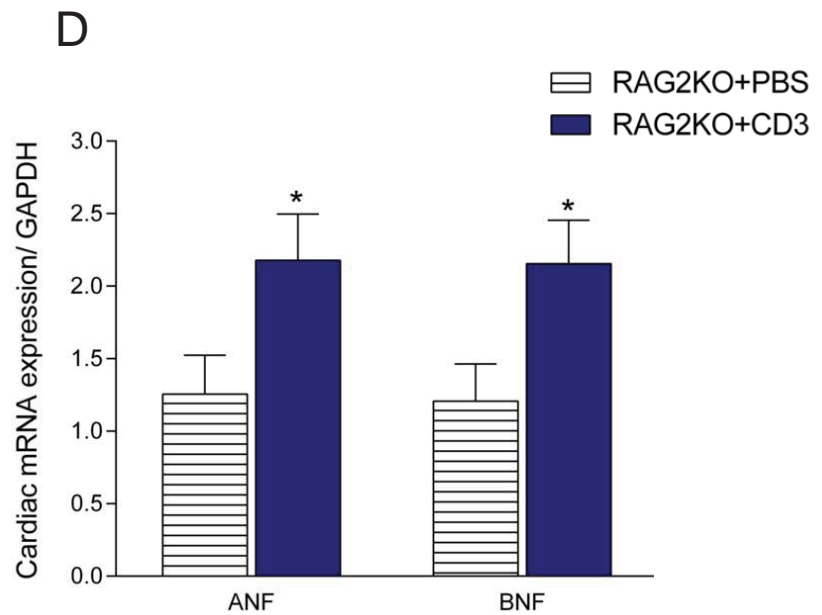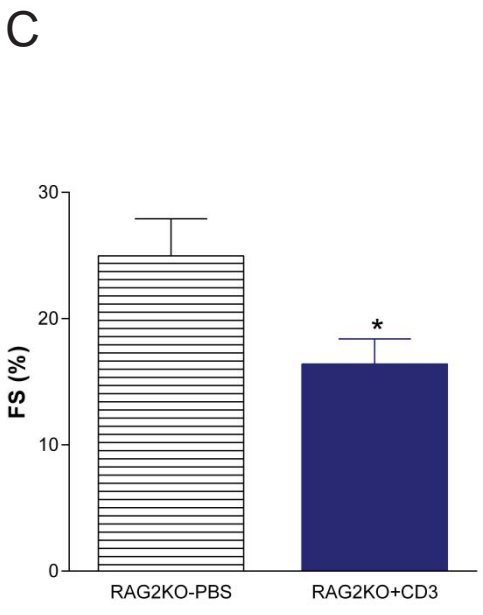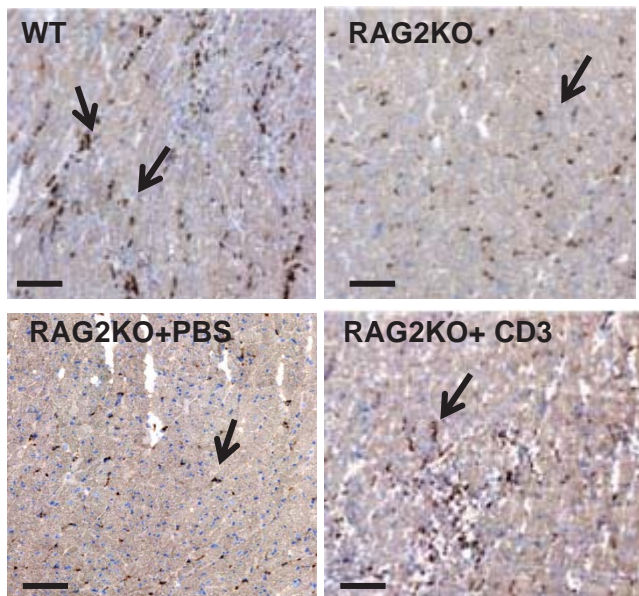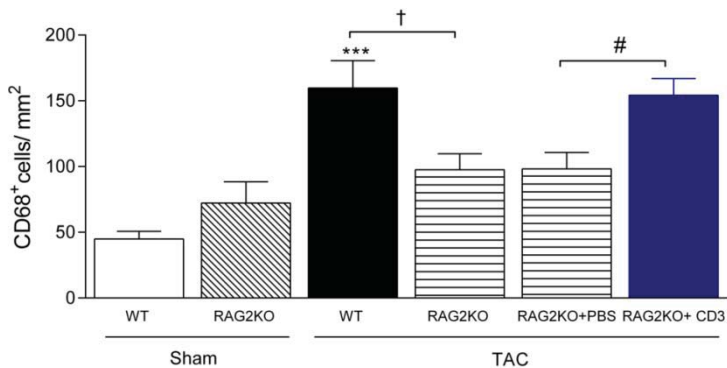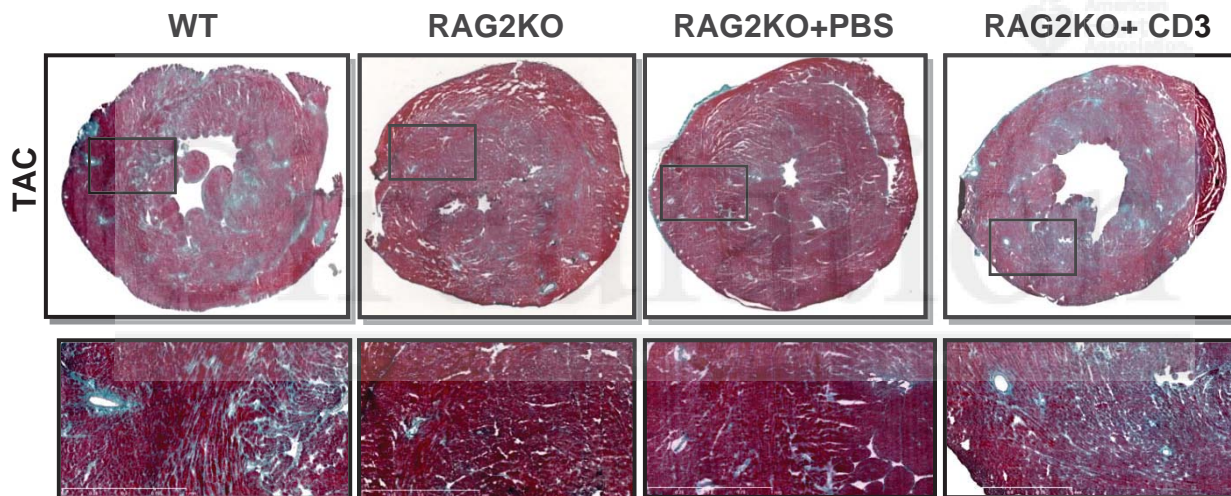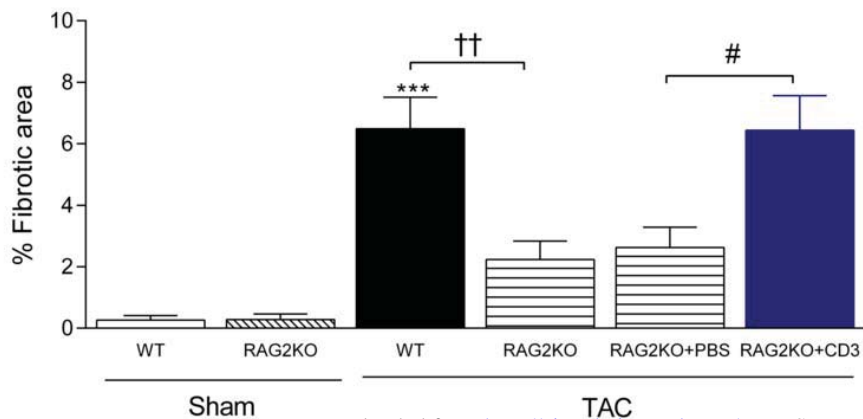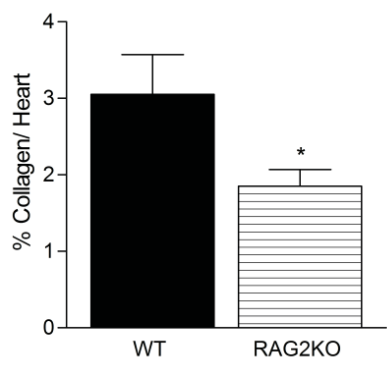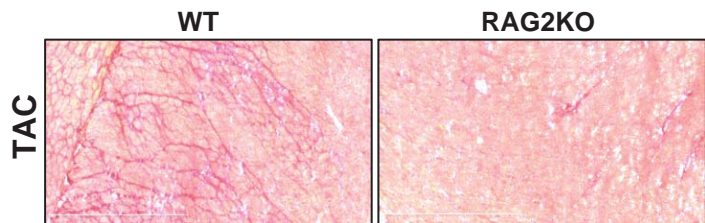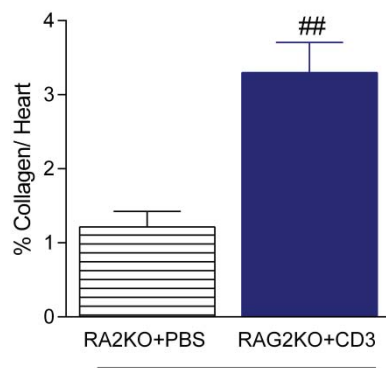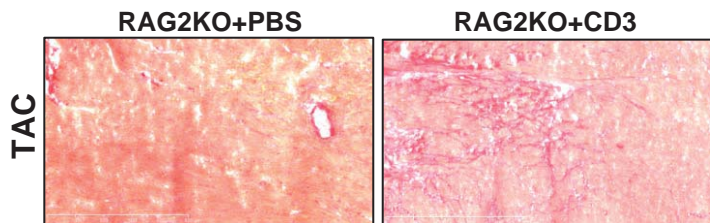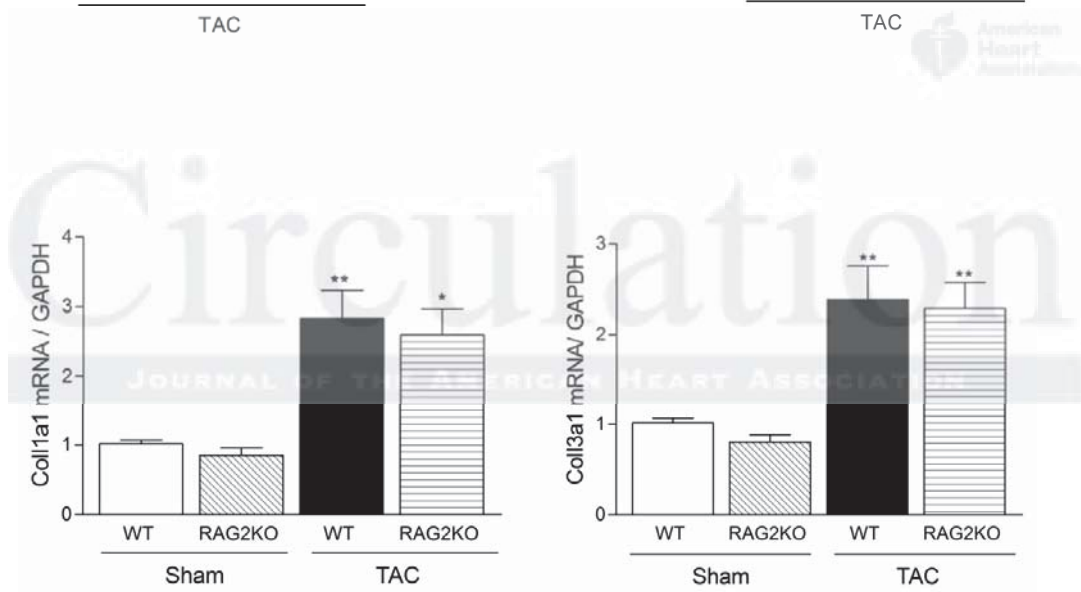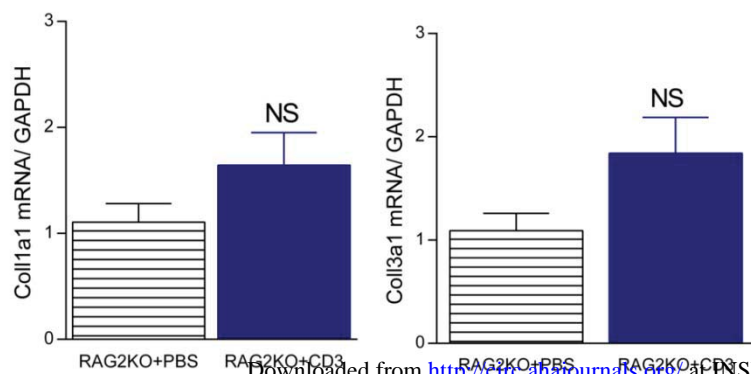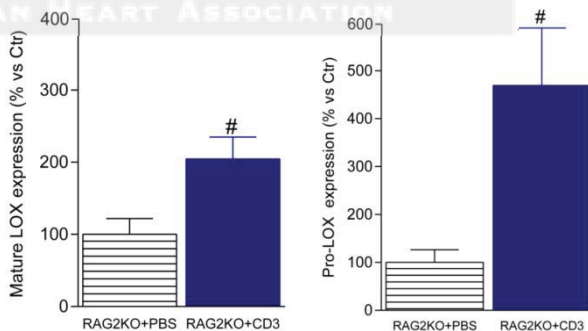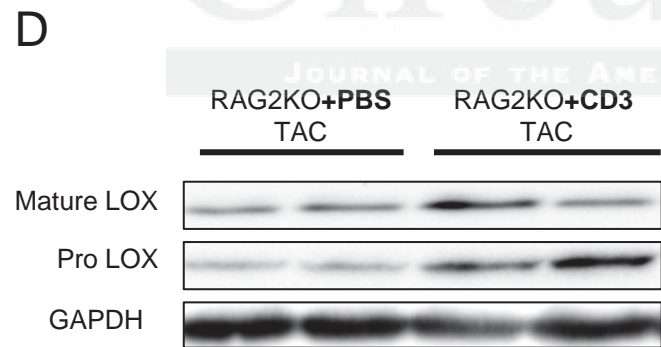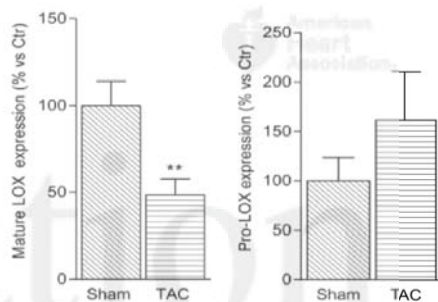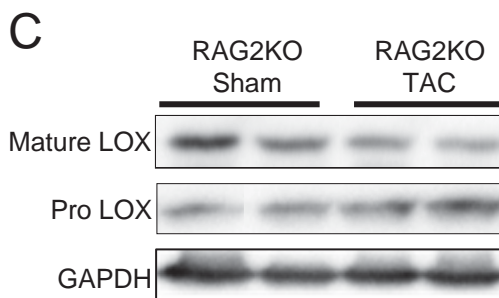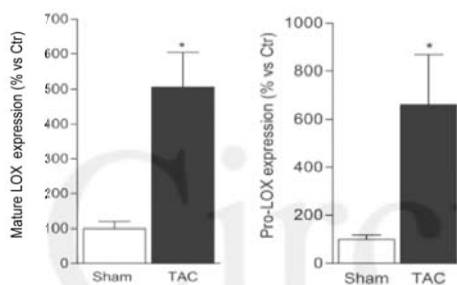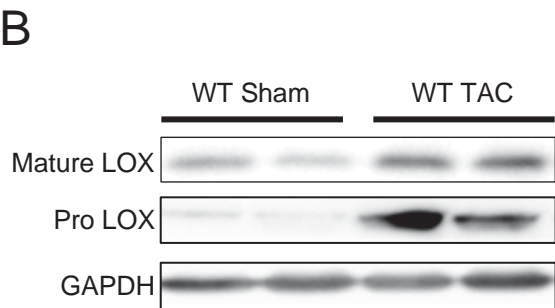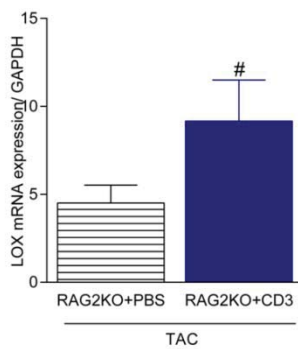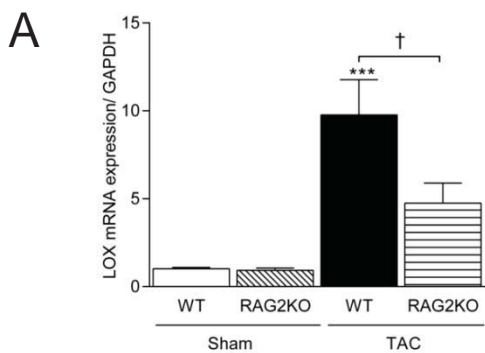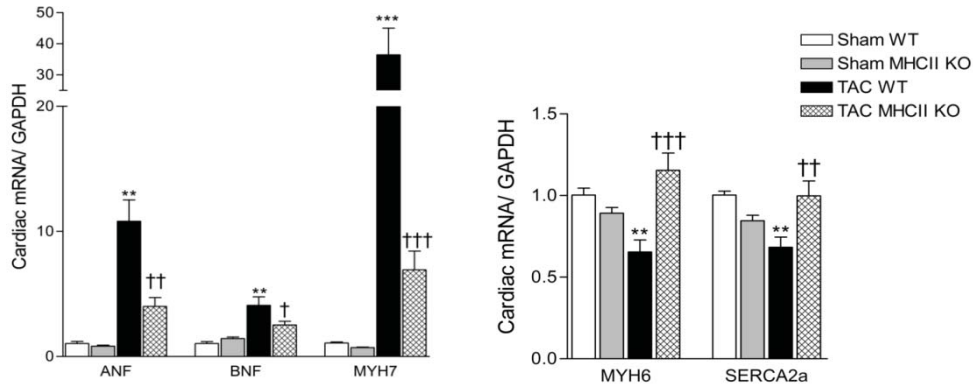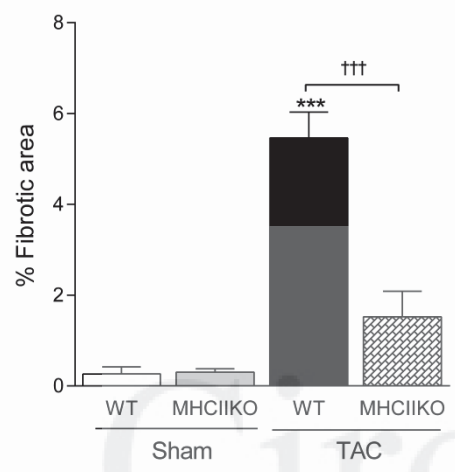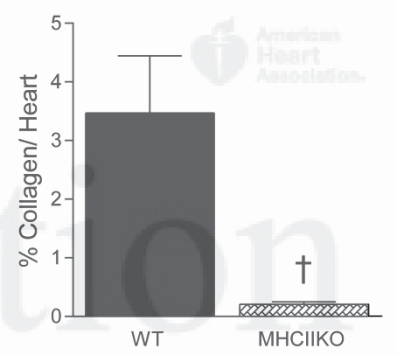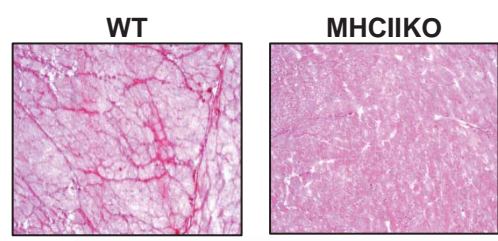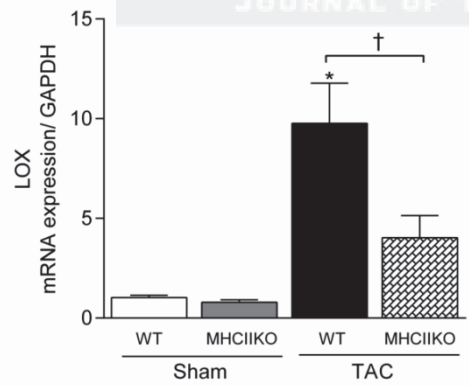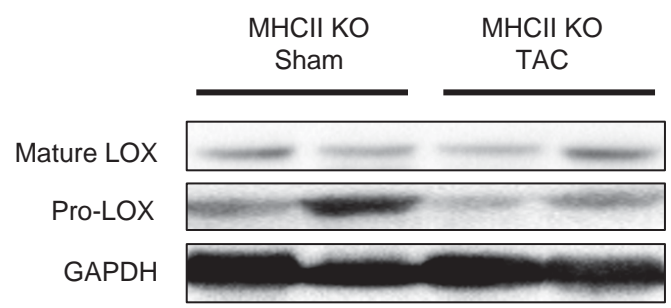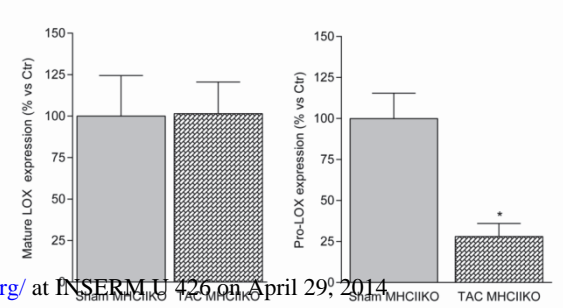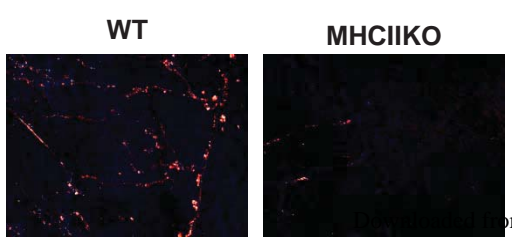
SUPPLEMENTAL MATERIAL

Supplemental Methods

Transverse aortic constriction

Mice were anesthetized with intraperitoneal ketamine (60 mg/kg) and xylazine (6 mg/kg). Anesthesia was maintained during chirurgical pro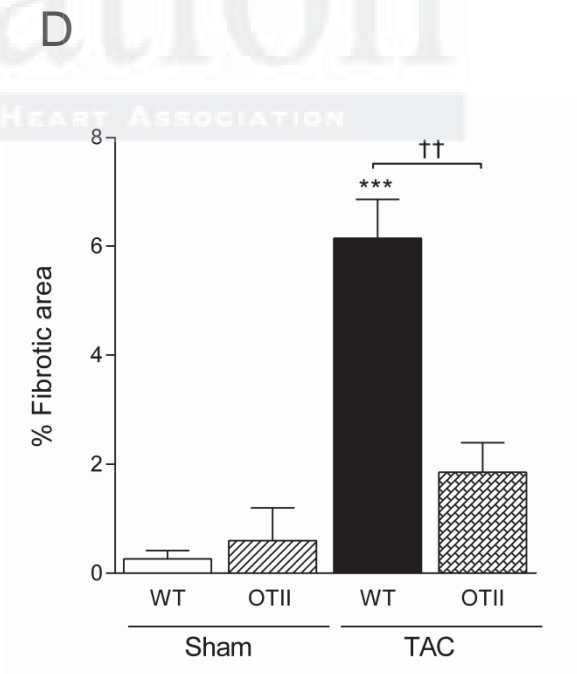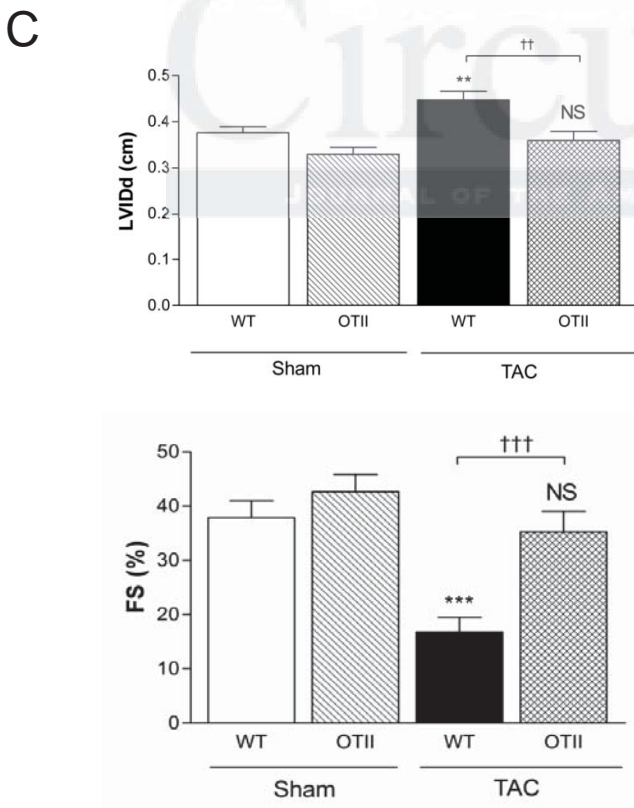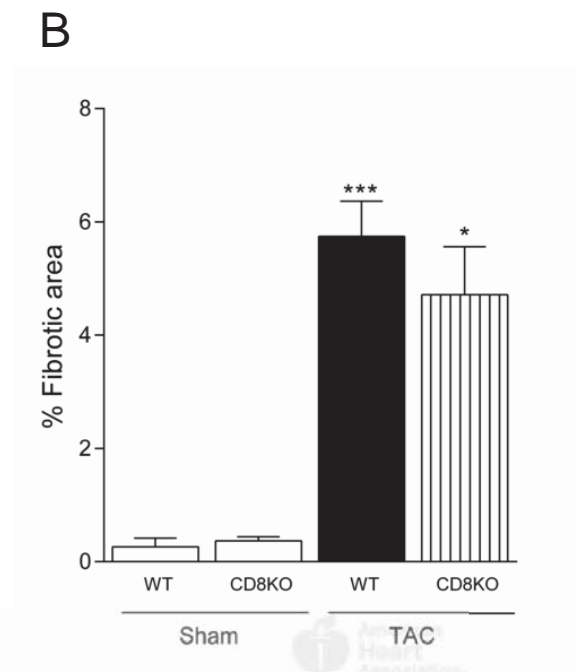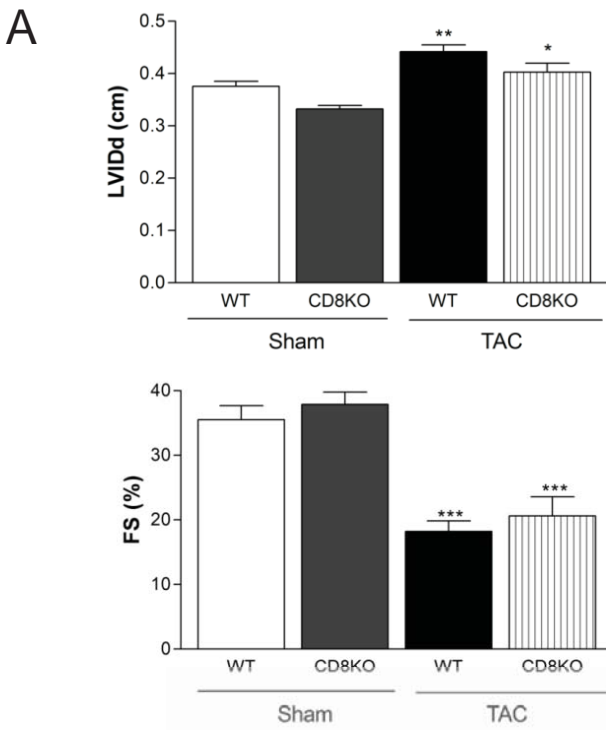cedure with isoflurane (1.5%). Transverse aortic constriction (TAC) was performed as previously described. [1] TAC was induced by ligation of the transverse aorta using a 7-0 Prolene suture. For this purpose, two knots of a 1.5 mm distance (26-gauge needle circumference) were made on the thread which was carefully introduced around the aorta. Both knots were tight together to perform constriction. Sham operated mice underwent the same surgery without constriction. Mice were sacrificed after 6 weeks of TAC. A single operator performed surgical procedures for all the experiments.

Echocardiography and hemodynamic measurements

Animals were anesthetized with 2% isoflurane and examined by trans-thoracic echocardiography (echocardiograph Vivid 7 ultrasound, GE) 6 weeks after surgery. Cardiac ventricular dimensions were measured on M-mode images as previously described.[1] The echocardiography operator was blinded to genotype and mice chirurgical procedure.

Real time PCR analysis

RNA was extracted using the Qiagen RNeasy Mini Kit from cardiac tissue according to the manufacturer's instructions. DNase treatment was systematically performed. Quality and quantification of extracted RNA were assessed by Experion analysis. The cDNA was synthesized using Superscript II First-Strand system (Invitrogen). The absence of contaminants was checked by RT-PCR assays of negative control samples in which the Superscript II was omitted. mRNA was analyzed by real-time PCR using PowerSYBR green (Life Technology) probe method and the primers listed in Supplemental Methods. Melting curve analysis was performed to ensure purity of the PCR products and relative quantification was determined using the comparative CT method with data normalized to GAPDH and calibrated to the average of control group (Sham WT unless otherwise notified).

Symbol	Sequence	gene
ANF	F:AAG-GCC-AAG-ACG-AGG-AAG-AAG, R: AGA-GTG-GGC-AGA-GAC-AGC-AAA	NM_008725.2
BNF	F: GAA GGT GCT GTC CCA GAT GAT T, R:GCT CTG GAG ACT GGC TAG GAC TT	NM_008726.4
MYH6	F: CCT AGC CAA CTC CCC GTT CT, R: GCC AAT GAG TAC CGC GTG A	NM_001164171.1
MYH7	F: TGA-GCC-TTG-GAT-TCT-CAA-ACG-T, R: AGG-TGG-CTC-CGA-GAA-AGG-AA	NM_080728.2
Coll1a1	F: AGC CTG AGT CAG CAG ATT GAG AA, R: TGG TTA GGG TCG ATC CAG TAC TCT	NM 007742.3
Coll3a1	F: ACGTAGATGAATTGGGATGCAG, R: GGGTTGGGCAGTCTAGTG	NM_009930.2
SERCA2a	F: TGCCCCCCTGGGAGAATA , R: CTGGAAAATGAGCGGCAAAG	AJ223584.1
LOX	F: CAGAGGAGAGTGGCTGAAGG, R: CCAGGACTCAATCCCTGTGT	NM_010728.2
CX3CL1	F: TGG-CTT-TGC-TCA-TCC-GCT-ATC-AG, R: CGT-CTG-TGC-TGT-GTC-GTC-TCC	NM_009142.3
CXCL10	F: ATG ACG GGC CAG TGA GAA TG, R: ATT CTT TTT CAT CGT GGC AAT GA	NM_021274.2
CCL17	F: TGT CCA GGGCAA GCT CAT CT, R: ATG CCT CAG CGG GAA GGT	NM_011332.3
CXCL16	F: CAA CCC TGG GAG ATG ACC AC, R: CTG TGT CGC TCT CCT GTT GC	NM_023158.6
GAPDH	F : ATGACTCCACTCACGGCAAATT, R : TCCCATTCTCGGCCTTGAC	NM_008084

Western Blotting

Mouse tissues were lysated using lysis buffer (50 mM Tris-HCl, pH 7.5, 150 mM NaCl, 1 mM EDTA, 1 mM EGTA, 1% Triton ×100) supplemented with complete protease inhibitor cocktail (Sigma). A 30-µg sample of total protein were loaded on a 12.5% polyacrylamide gel and transferred to PVDF membrane. The membrane was blocked with 1% BSA in TBS-Tween 20 (0.1%) for 1h. A specific rabbit polyclonal antibody against lysyl oxidase (Thermo Scientific) was used (1:500). Bands were detected by peroxidase conjugated secondary antibodies (Cell Signaling) and visualized with the ECL chemiluminescence system (GE Healthcare). Proteins were detected using an automatic densitometer (Chemidoc, Bio-Rad). The blots were also probed with a monoclonal GAPDH antibody (Cell Signaling) as a control for loading.

Immunohistology

To wash out blood cells from cardiac coronary vessels, we injected 5 ml of PBS in cardiac ventricles before removing heart from anesthetized animals. Cardiac tissues were frozen in OCT tissue embedding compound (Tissue Tek, EMS) at -80°C. For immunohistology staining, cryosections of 5µm were fixed with cold acetone. Endogenous biotin and background peroxidase were blocked (Avidin/Biotin Blocking kit from Vector Labs and peroxidase blocking buffers from Dako). Sections were stained using Vectastain Elite ABC Kit (Vector) and colorimetric detection was visualized using

DAB substrate. Finally, sections were counterstained with hematoxylin, dehydrated, mounted and digitized with a Hamamatsu NanoZoomer.

The antibodies used for histology staining were as follows: anti-CD68 (clone FA-11, AbD serotec) and anti-CD3e (clone 145-2C11, AbD serotec).

Immunofluorescence

Cryosections of 5μm were blocked using the Avidin/Biotin blocking kit (Vector Labs) followed by 2% normal goat serum (Sigma-Aldrich) and 1% BSA in PBS. Sections were stained overnight with rat anti-mouse CD45 (clone 30-F11, BD Pharmingen), CD4 (clone GK 1.5, eBioscience) or CD8α (clone 53-6.7, eBioscience) and hamster anti-mouse CD3 followed by staining with secondary antibody: anti-rat DL488 and anti-hamster-Biotin/Streptavidin DL549. Nuclei were stained by DAPI.

Histological Staining Methods

Cryosections of 10μm were stained with Masson's trichrome and picrosirius red in order to assess cardiac fibrosis and collagen content. Three sections per heart were stained and digitized with a Hamamatsu NanoZoomer. Finally, stained areas and total surface from each section were determined using color-based thresholding and quantified by ImageJ software. To assess collagen fibers, picrosirius red stained sections were studied under polarized light.

Reconstitution of T cell populations into RAG2KO recipient mice before TAC

Spleens of control WT mice were flushed with cold PBS and erythrocytes were eliminated using ACK lysis buffer. Splenic CD3$^+$ T cells were isolated by immunomagnetic selection (EasySep CD3-negative selection kit, StemCell Technologies). T cell purity was routinely greater than 90%. RAG2KO recipient mice were injected with T cells ($2x10^7$ cells in a volume of 250 μl) or PBS into the left external jugular vein. Two weeks after injection, RAG2KO+CD3 and control RAG2KO+PBS mice underwent TAC.

***Ex vivo* re-stimulation of T cells**

For cytokine production measurements, $5×10^5$ mediastinal lymph nodes cells were stimulated in 500μl RPMI supplemented with 5% FBS, non essential amino acid and 50μM β-mercaptoethanol per well in 48-well plates. T cells were stimulated with 1.5 μg/ml of anti-CD3 and anti-CD28 mAb (BioLegend).

Levels of IL-2 were evaluated after 12h and levels of IL-4 and IFNγ after 48h, using enzyme-linked immunosorbent assay (ELISA, eBioscience) kits according to the manufacter's instructions. The absorbance was measured at 450 and 570 nm.

Intracellular cytokine assay

Mediastinal lymph nodes cells (2×10^6 /ml) were resuspended in RPMI supplemented with 5% FBS, non essential amino acid and 50µM β-mercaptoethanol per well in 24-well low-adherence plates. Cells were stimulated with phorbol ester (PMA 50 ng/ml) and calcium ionophore (ionomycin 1 µg/ml) for 4 hours. Brefeldin A was added during the last 2 hours (10 µg/ml). Cells were stained for surface expression, fixed, and permeabilized using Cytofix/Cytoperm kit (BD Biosciences) and stained for intracellular IFNγ and IL-4 before analysis on LSRII.

Isolation of cardiac immune cells

The hearts were cut into pieces and digested in RPMI containing 0.12 mg/ml of Liberase TM (Roche) for 10 min at 37°C with vigorous stirring. The supernatant was then added to 10 ml of ice-cold RPMI supplemented with 10% of heart inactivated fetal bovine serum (FBS). Two milliliters of fresh digesting solution was added to the remaining tissue fragments. Cell suspensions were pooled and erythrocytes were lysed by using ACK lysis buffer. Cell suspensions were stained for flow cytometry analysis.


Flow cytometry

Spleens were flushed and crushed in cold PBS and erythrocytes were removed by using ACK lysis buffer. Then, spleen, lymph node and cardiac cell suspensions were passed through a 40µm strainer. Fc receptors were blocked with 5 µg/ml of anti-mouse CD16/CD32 in PBS containing 4% FBS and 2mM EDTA for 20 min at 4°C. Cells were stained with mixtures of antibodies for 30 min at 4°C then incubated with Live/dead Yellow fluorescent reactive dye (Invitrogen) dead staining kit accordingly to the manufacturer's instruction before fixation with PFA (1%). Cardiac cell numbers were quantified using CountBright absolute counting beads (Life Technologies). Prior to acquisition, cells were resuspended in PBS/FBS/EDTA solution. For cardiac cell suspensions, 52 000 beads were added in each cardiac cell samples before acquisition. Flow cytometric multiparameter acquisition was

performed on a LSR II (Digital LSR II; BD Biosciences) and data were analyzed with FlowJo 7.6.3 software (Tree Star).

Cells were stained with directly conjugated Abs against: CD4 APC/Cy7 (clone RM4-5), CD8α PB (clone 53-6.7), IFNγ PE (clone XMG1.2), IL-4 AF647 (clone 11B11), CD45 PE/Cy7 (clone 30-F11), CD3$_\varepsilon$ FITC (clone 145-2C11), B220 APC (clone RA3-6B2), TCR$_\beta$ PerCP-Cy5.5 (clone H57-597), CD44 PE (clone IM7), CD11b PE (clone M1/70), CD11c PECy7 (clone N418), MHCII PerCPCy5.5 (clone M5/114.15.2) and matching isotype controls from eBioscience and BioLegend. CD16/CD32 for Fc blocking was from eBioscience.
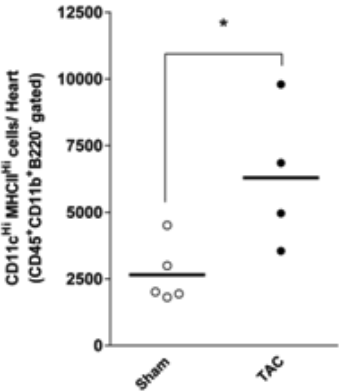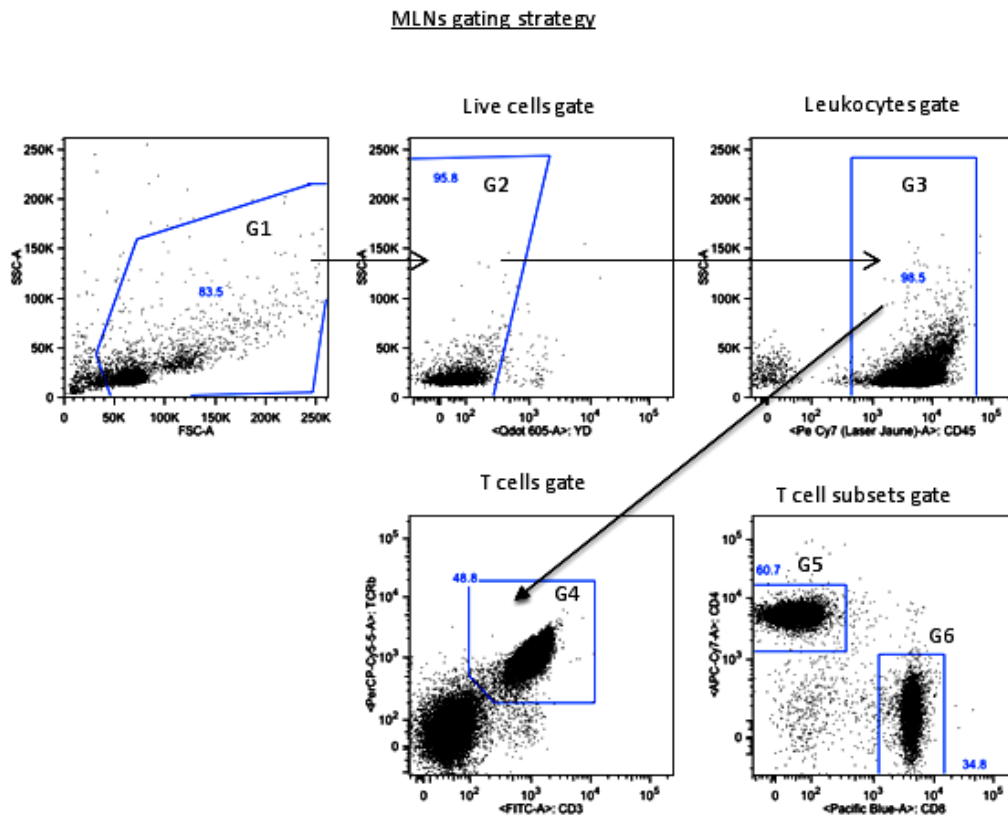
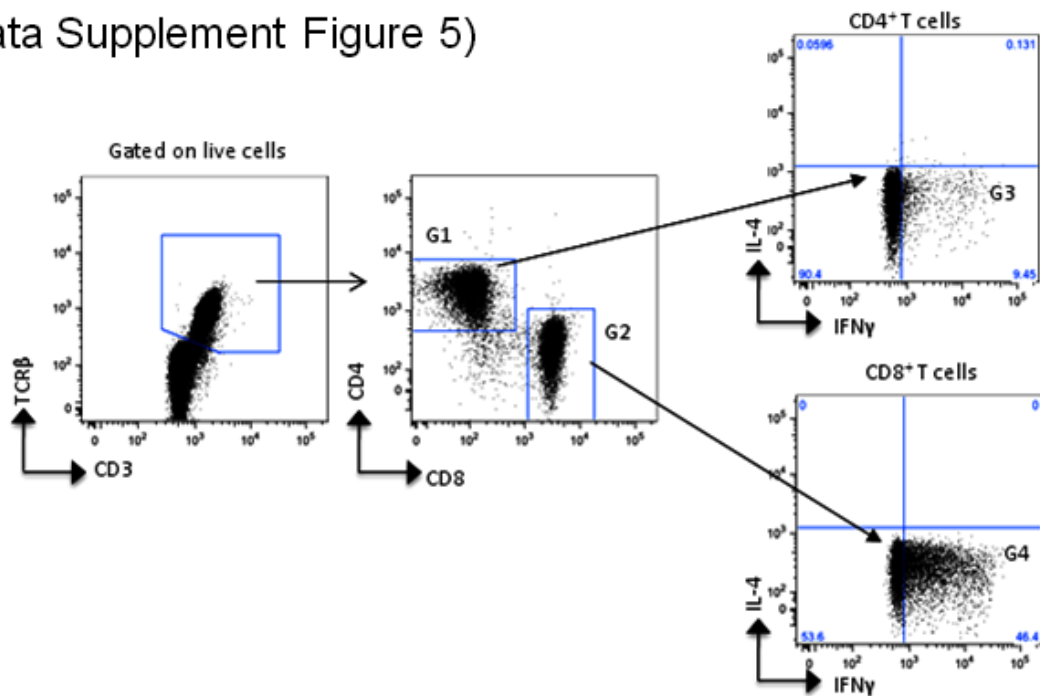**Supplemental Figures**

(Data Supplement Figure 1)

Heart gating strategy
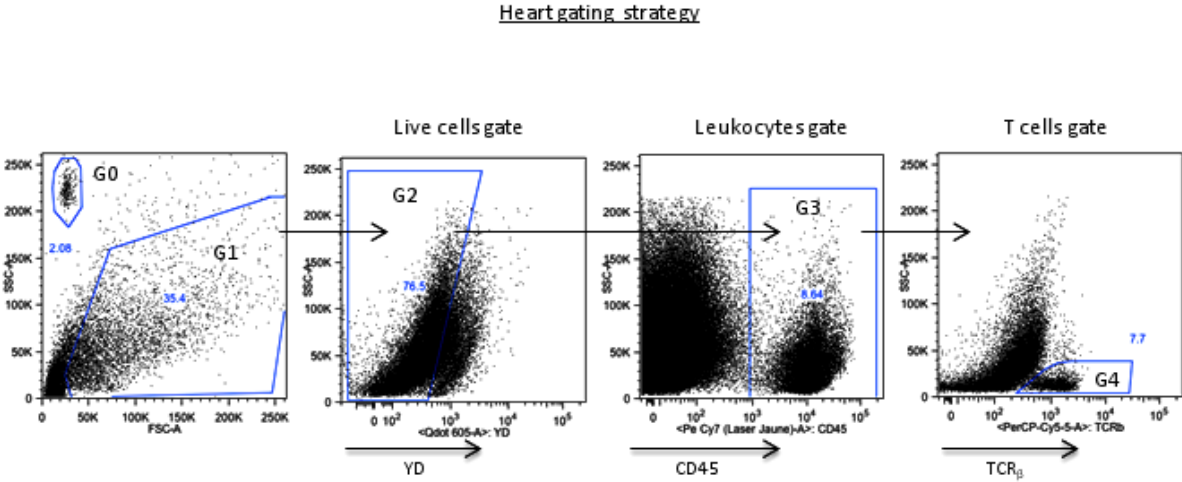
(Data Supplement Figure 2)
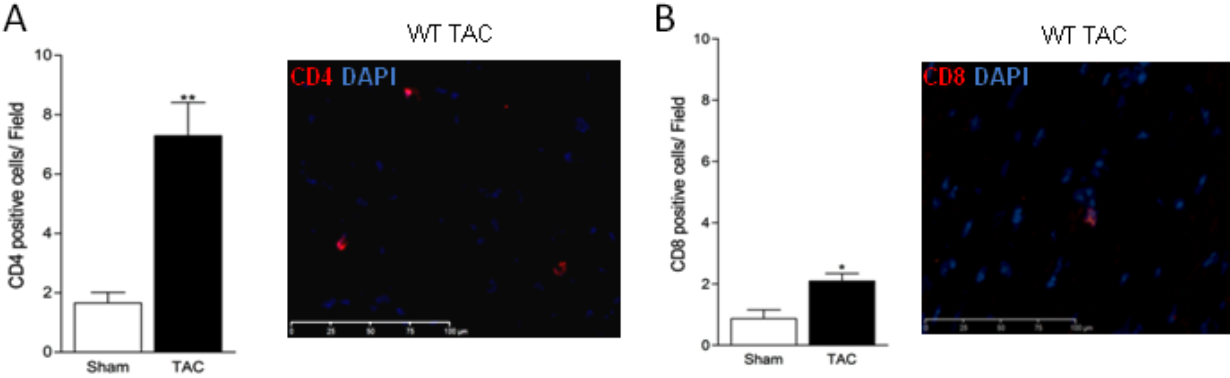
(Data Supplement Figure 3)

(Data Supplement Figure 4)
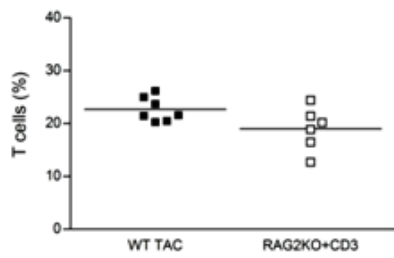
MLNs gating strategy

(Data Supplement Figure 5)

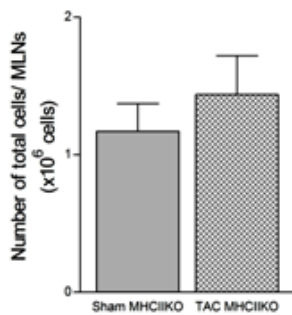## (Data Supplement Figure 6)

A

Repopulation of T cells in RAG2KO mice

B

	RAG2KO +PBS TAC n=7	RAG2KO +CD3 TAC n=6	P
IVSd (cm)	0.128±0.009	0.122±0.009	NS
LVPWd (cm)	**0.114±0.008**	**0.113±0.007**	**NS**
LVIDd (cm)	0.393±0.017	0.413±0.007	NS
LVIDs (cm)	**0.295±0.022**	**0.343±0.010**	**NS**
EDV (ml)	0.160±0.020	0.175±0.008	NS
ESV (ml)	**0.073±0.012**	**0.105±0.009**	**NS**
FS (%)	24.97±3.40	16.39±2.00	*
HR (BMP)	**555±20**	**603±6**	**^**

(Data Supplement Figure 7)

A

B
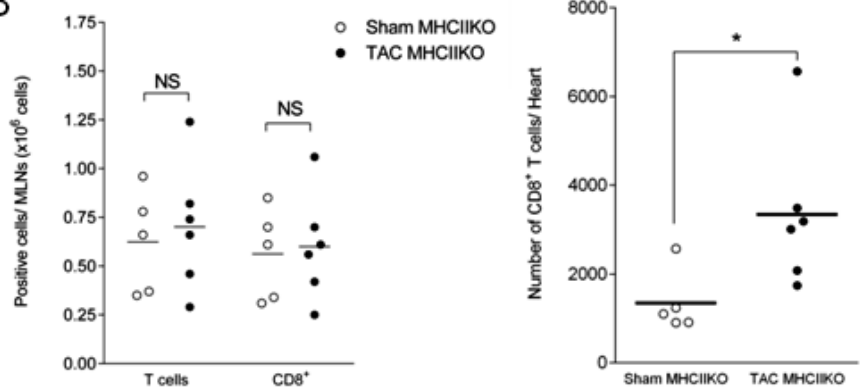
(Data Supplement Figure 8)

A

B

(Data Supplement Figure 9)

A

B
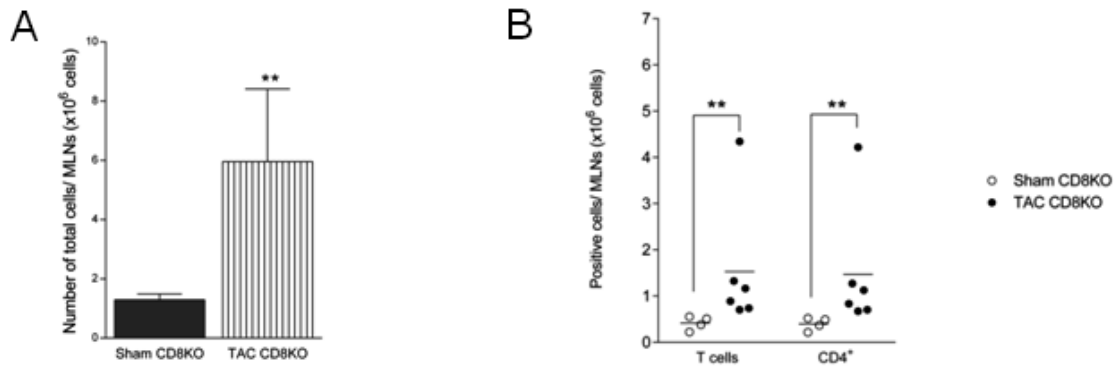
(Data Supplement Figure 10)
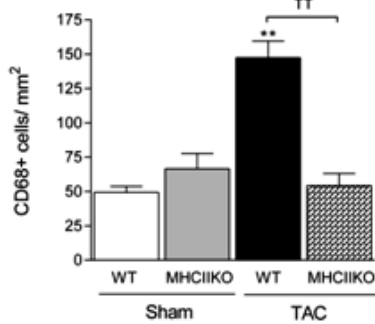
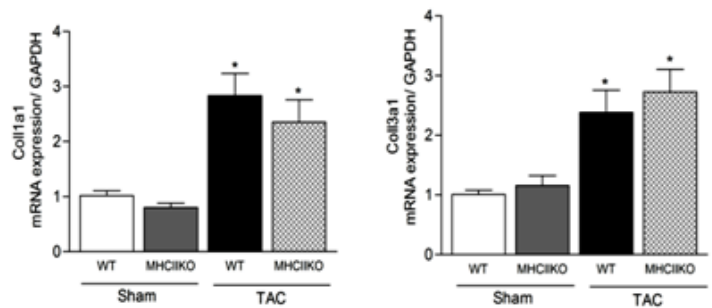|	WT Sham n=7	WT TAC n=13	P	CD8KO Sham n=5	CD8KO TAC n=8	P
IVSd (cm)	0,088±0.004	0,110±0.004	***	0,083±0.006	0,129±0.006	***,†
LVPWd (cm)	0,082±0.003	0,103±0.004	**	0,093±0.006	0,123±0.005	**,††
LVIDd (cm)	0,378±0.004	0,442±0.011	**	0,330±0.006	0,388±0.017	*, NS
LVIDs (cm)	0,236±0.006	0,356±0.018	***	0,205±0.008	0,307±0.017	*, NS
EDV (ml)	0,134±0.004	0,225±0.022	**	0,092±0.005	0,160±0.020	NS,†
ESV (ml)	0,036±0.003	0,126±0.018	***	0,022±0.005	0,096±0.015	*, NS
FS (%)	37,68±1.56	19,34±1.68	***	37,87±1.53	20,63±2.76	***, NS
HR (BMP)	538±27	535±20	NS	605±10	630±11	NS, ††

(Data Supplement Figure 11)
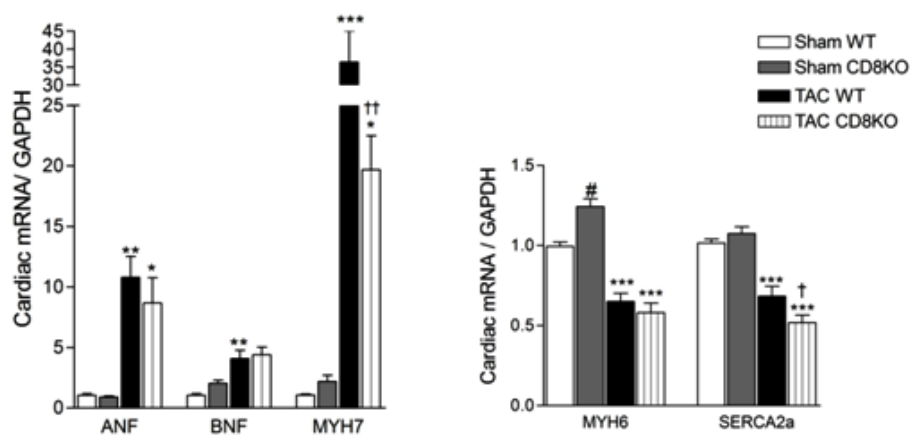
(Data Supplement Figure 12)

(Data Supplement Figure 13)

A

B

CD8KO TAC
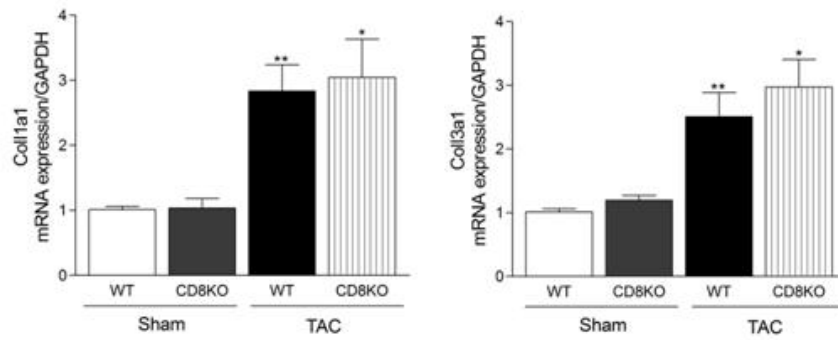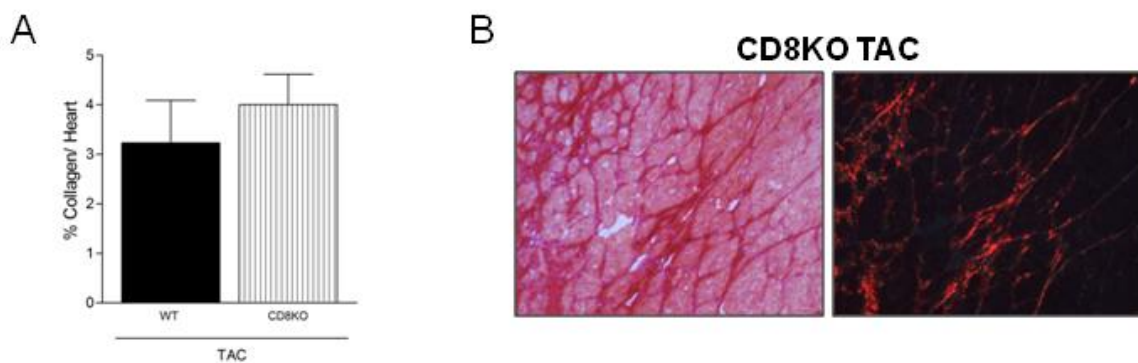
(Data Supplement Figure 14)

	WT Sham n=9	WT TAC n=8	*P*	OTII Sham n=4	OTII TAC n=8	*P*
IVSd (cm)	0.090±0.002	0.117±0.004	**	0.085±0.006	0.128±0.006	**, NS
LVPWd (cm)	0.090±0.005	0.125±0.013	*	0.097±0.007	0.133±0.008	*, NS
LVIDd (cm)	0.376±0.012	0.448±0.018	**	0.347±0.013	0.360±0.019	NS, ††
LVIDs (cm)	0.240±0.015	0.374±0.024	***	0.197±0.011	0.239±0.024	NS, †††
EDV (ml)	0.146±0.014	0.229±0.026	**	0.110±0.010	0.125±0.017	NS, ††
ESV (ml)	0.041±0.007	0.141±0.024	***	0.0222±0.004	0.044±0.012	NS, †††
FS (%)	37.90±3.11	16.82±2.63	***	42.80±3.36	35.25±3.77	NS, †††
HR (BMP)	623±33	674±31	NS	646±20	629±18	NS, NS

Figure Legends

Data Supplement Figure 1. Flow cytometry gating strategy to quantify T cells within cardiac tissue. Cells are first gated (G1) on a forward scatter/side scatter (FSC-A/SSC-A) dot plot and live cells are selected (G2). Cells from G2 are further characterized by the expression of CD45 (leukocytes, G3). Finally, T cells are first identified in TCR_β-positive cells (G4) and further analysed for $CD3_\varepsilon$ and CD4 or CD8 expression. Countbright beads are identified by their FSC-A/SSC-A parameters (G0) and are used to normalize cell acquisition numbers.

Data Supplement Figure 2. Accumulation of CD4$^+$ and CD8$^+$ T cells within cardiac tissue of wild type mice after 6 weeks of TAC. (A) Quantification and representative immunofluorescence of CD4$^+$ T cells and (B) CD8$^+$ T cells in cardiac tissue (red color) of Sham and mice submitted to TAC (n=5). Nuclei were stained by DAPI (blue color). Values shown are mean±SEM. Significance vs Sham: *P<0.05, **P<0.01 by U test.

Data Supplement Figure 3. Accumulation of dendritic cells into cardiac tissue of mice after 6 weeks of TAC. Quantification by flow cytometry analysis of the number of dendritic cells within cardiac tissue of Sham and TAC animals (n=4). Dendritic cells were defined in CD45$^+$ B220$^-$ population as cells expressing CD11b and high level of CD11c and MHCII molecules. Results were expressed in number of cells per heart. Values shown are mean±SEM. Significance vs Sham: *P<0.05 by U test.

Data Supplement Figure 4. Flow cytometry gating strategy to quantify T cell subsets within mediastinal draining lymph nodes (MLNs). Cells are first gated (G1) on a forward scatter/side scatter (FSC-A/SSC-A) dot plot and live cells are selected (G2). Cells from G2 are further characterized by the expression of CD45 (leukocytes, G3). Finally, T cells are gated on $CD3_\varepsilon$$^+$ $TCR_\beta$$^+$ double positive cells (G4) and T cell subsets are defined by CD4 (G5) or CD8 (G6) expression.

Data Supplement Figure 5. **Flow cytometry gating strategy to quantify T cells expressing IFNγ or IL-4 after *ex vivo* stimulation.** After gating on live cells, T cells are gated on CD3$^+$ TCR$_\beta$$^+$ double positive cells and T cell subsets are defined on CD4 (G1) or CD8 (G2) expression. IFNγ positive CD4$^+$ T cells were identified in G3 and IFNγ positive CD8$^+$ T cells in G4.

Data Supplement Figure 6. Transfer of T cells into RAG2KO recipient mice reestablishes the presence of T cells in spleen with similar level to WT after TAC. Echocardiographic parameters after reconstitution of T cell compartment. (A) Percentage of CD3$^+$TCR-β$^+$ cells in spleen of WT and RAG2KO+CD3 mice after TAC was expressed as percentage of CD45$^+$ cells (n=6-7). (B) Echocardiographic parameters of RAG2KO+PBS and RAG2KO+CD3 mice after TAC. IVSd indicates diastolic interventricular septal wall thickness; LVPWd**,** diastolic left posterior wall thickness**;** LVIDd, diastolic left ventricular dimension; LVIDs, systolic left ventricular dimension**;** EDV, end diastolic volume; ESV, end systolic volume; FS, fractional shortening and HR, heart rate. Values shown are mean±SEM. Significance vs RAG2KO+PBS: *P<0.05 by *t* test. NS for not significant.

Data Supplement Figure 7. No changes in cellularity of MLNs isolated from mice lacking CD4$^+$ T cells (MHCIIKO mice) after transverse aortic constriction (TAC). Accumulation of CD8$^+$ T cells within cardiac tissue of MHCIIKO mice after TAC. (A) Quantification of total cellular density (left panel), T cells and CD8$^+$ T cell subsets densities (right panel) in MLNs expressed as cell number per MLNs isolated from MHCIIKO Sham and TAC operated mice (n=6). (B) Quantification by flow cytometry analysis of CD8$^+$ T cells within heart of Sham and TAC MHCIIKO mice (n=6). CD8$^+$ T cells were expressed as number of cell per heart. Values shown are mean±SEM. Significance vs Sham: *P<0.05 by *U* test.

Data Supplement Figure 8. Mice lacking CD4$^+$ T cells (MHCIIKO) exhibit less macrophage accumulation and no modification of procollagen genes expression as compared to WT after 6 weeks of transverse aortic constriction (TAC). (A) Quantification of CD68 positive cells per mm^2 in WT and MHCIIKO mice (n=8). (B) Cardiac mRNA expression of type I and III procollagens (Coll1a1 and Coll3a1) in WT and MHCIIKO mice (n=6-13 per group). Data were normalized to GAPDH and

calibrated to the average of WT Sham. Values shown are mean±SEM. Significance vs Sham: *$P<0.05$, **$P<0.01$. Significance vs WT TAC: [††]$P<0.01$ by ANOVA.

Data Supplement Figure 9. MLNs isolated from mice lacking CD8^{+} T cells (CD8KO) exhibit higher density of CD4^{+} T lymphocytes. (A) Quantification of cellular density of MLNs expressed as cell number per MLNs isolated from Sham and TAC operated mice (n=4-6). (B) Quantification by flow cytometry analysis of $CD3^+TCR_\beta^+$ double positive cells (defined T cells) and CD4^{+} T cells. Results were expressed in number of cells per MLNs. Values shown are mean±SEM. Significance vs Sham CD8KO: **$P<0.01$ by U test.

Data Supplement Figure 10. After 6 weeks of transverse aortic constriction (TAC), mice lacking CD8^{+} T cells (CD8KO) develop cardiac dilation and dysfunction compared to Sham. Echocardiographic parameters of WT Sham, WT TAC, CD8KO Sham and CD8KO TAC. IVSd indicates diastolic interventricular septal wall thickness; LVPWd, diastolic left posterior wall thickness; LVIDd, diastolic left ventricular dimension; LVIDs, systolic left ventricular dimension; EDV, end diastolic volume; ESV, end systolic volume; FS, fractional shortening and HR, heart rate. Values shown are mean±SEM. Significance vs Sham: *$P<0.05$, **$P<0.01$, ***$P<0.001$, Significance vs WT TAC: [†]$P<0.05$, [††]$P<0.01$ by ANOVA. NS for not significant.

Data Supplement Figure 11. Absence of CD8^{+} T cell (CD8KO mice) prevents fetal genes activation induced by TAC. Cardiac mRNA expression of the atrial and brain natriuretic peptides (ANF, BNF) as well as the α and β myosin heavy chain (MYH6, MYH7) and the sarco(endo) plasmic reticulum Ca^{2+}-ATPase (SERCA2a) in WT and CD8KO mice (Sham, n=4; TAC, n=8) mRNA expression was normalized to GAPDH and represented as fold change to WT Sham. Values shown are mean±SEM. Significance vs Sham: *$P<0.05$, **$P<0.01$, ***$P<0.001$; significance vs WT TAC: [†]$P<0.05$, [††]$P<0.01$. Significance vs Sham WT: [#]$P<0.05$ by ANOVA.

Data Supplement Figure 12. Mice lacking CD8^{+} T cells (CD8KO) exhibit no modification of procollagen genes expression compared to WT after transverse aortic constriction (TAC). Cardiac mRNA expression of type I and III procollagens (Coll1a1 and Coll3a1) in WT and CD8KO

mice (n=4-8 per group). Data were normalized to GAPDH and calibrated to the average of WT Sham. Values shown are mean±SEM. Significance vs Sham: *P<0.05, **P<0.01 by ANOVA.

Data Supplement Figure 13. Mice lacking CD8+ T cells (CD8KO) exhibit no modification of collagen content and cross-linking after transverse aortic constriction (TAC) compared to WT TAC. (A) Quantification of total collagen deposition in cardiac tissue of WT and CD8KO mice submitted to TAC based on picrosirius red staining viewed under white light (n=4-8). (B) Representative cardiac tissue of CD8KO mice submitted to TAC, stained with picrosirius red staining and viewed under white (left) and polarized (right) light (x200). Values shown are mean±SEM.

Data Supplement Figure 14. After 6 weeks of transverse aortic constriction (TAC), OTII mice did not develop cardiac dilation and dysfunction compared to Sham. Echocardiographic parameters of WT Sham, WT TAC, OTII Sham and OTII TAC. IVSd indicates diastolic interventricular septal wall thickness; LVPWd, diastolic left posterior wall thickness; LVIDd, diastolic left ventricular dimension; LVIDs, systolic left ventricular dimension; EDV, end diastolic volume; ESV, end systolic volume; FS, fractional shortening and HR, heart rate. Values shown are mean±SEM. Significance vs Sham: *P<0.05, **P<0.01, ***P<0.001, Significance vs WT TAC: ††P<0.01, †††P<0.001 by ANOVA. NS for not significant.

Supplemental References

1-   Lairez O, Calise D, Bianchi P, Ordener C, Spreux-Varoquaux O, Guilbeau-Frugier C, Escourrou G, Seif I, Roncalli J, Pizzinat N, Galinier M, Parini A, Mialet-Perez J. Genetic deletion of MAO-A promotes serotonin-dependent ventricular hypertrophy by pressure overload. *J Mol Cell Cardiol.*2009; 46:587-595